Article

Thermodynamics, Kinetics, and Mechanism of (silox)M(olefin) to (silox)M(alkylidene) Rearrangements (silox = BuSiO; M = Nb, Ta)

Kurt F. Hirsekorn, Adam S. Veige, Michael P. Marshak, Yelena Koldobskaya, Peter T. Wolczanski, Thomas R. Cundari, and Emil B. Lobkovsky

J. Am. Chem. Soc., **2005**, 127 (13), 4809-4830• DOI: 10.1021/ja046180k • Publication Date (Web): 10 March 2005

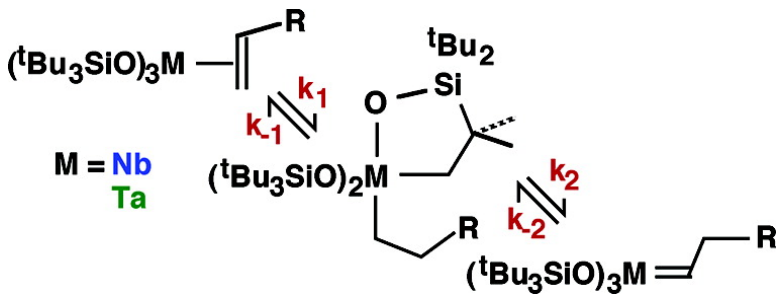

More About This Article

Additional resources and features associated with this article are available within the HTML version:

- Supporting Information
- Links to the 13 articles that cite this article, as of the time of this article download
- Access to high resolution figures
- Links to articles and content related to this article
- Copyright permission to reproduce figures and/or text from this article

View the Full Text HTML

J|A|C|S
ARTICLES
Published on Web 03/10/2005

Thermodynamics, Kinetics, and Mechanism of $(silox)_3M(olefin)$ to $(silox)_3M(alkylidene)$ Rearrangements ($silox = {}^tBu_3SiO$; M = Nb, Ta)

Kurt F. Hirsekorn,[†] Adam S. Veige,[†] Michael P. Marshak,[†] Yelena Koldobskaya,[†] Peter T. Wolczanski,*[,†] Thomas R. Cundari,[‡] and Emil B. Lobkovsky[†]

Contribution from the Department of Chemistry and Chemical Biology, Baker Laboratory, Cornell University, Ithaca, New York 14853, and Department of Chemistry, University of North Texas, Box 305070, Denton, Texas 76203-5070

Received June 28, 2004; E-mail: ptw2@cornell.edu

Abstract: Olefin complexes $(silox)_3M(ole)$ ($silox = {}^tBu_3SiO$; M = Nb (**1**-ole), Ta (**2**-ole); ole = C_2H_4, C_2H_3Me, C_2H_3Et, $C_2H_3C_6H_4$-*p*-X (X = OMe, H, CF_3), $C_2H_3{}^tBu$, $^cC_5H_8$, $^cC_6H_{10}$, $^cC_7H_{10}$ (norbornene)) rearrange to alkylidene isomers $(silox)_3M(alk)$ (M = Nb (**1**═alk), Ta (**2**═alk); alk = CHMe, CHEt, CH^nPr, $CHCH_2C_6H_4$-*p*-X (X = OMe, H, CF_3 (Ta only)), $CHCH_2{}^tBu$, $^cC_5H_8$, $^cC_6H_{10}$, $^cC_7H_{10}$ (norbornylidene)). Kinetics and labeling experiments suggest that the rearrangement proceeds via a δ-abstraction on a silox CH bond by the β-olefin carbon to give $(silox)_2RM(\kappa^2\text{-}O,C\text{-}OSi^tBu_2CMe_2CH_2)$ (M = Nb (**4**-R), Ta (**6**-R); R = Me, Et, ^{n}Pr, ^{n}Bu, $CH_2CH_2C_6H_4$-*p*-X (X = OMe, H, CF_3 (Ta only)), $CH_2CH_2{}^tBu$, $^cC_5H_9$, $^cC_6H_{11}$, $^cC_7H_{11}$ (norbornyl)). A subsequent α-abstraction by the cylometalated "arm" of the intermediate on an α-CH bond of R generates the alkylidene **1**═alk or **2**═alk. Equilibrations of **1**-ole with ole′ to give **1**-ole′ and ole, and relevant calculations on **1**-ole and **2**-ole, permit interpretation of all relative ground and transition state energies for the complexes of either metal.

Introduction

While the field of organometallic chemistry boasts a number of unique processes, the olefin metathesis reaction—and its heterogeneous analogue—is perhaps the most widespread in terms of application.[1] Commodity chemicals, polymers, and fine chemicals are all prepared via judicious use of alkene metathesis.[1−8] Surfactant and plasticizer production via the shell higher olefins process employs olefin cross metathesis to generate aldehyde and alcohol precursors from internal olefins that are too short or long.[2−5,9,10] The disproportionation of propene in the Philips triolefin process affords butene and ethylene, which is the more useful alkene.[2−5] Extension of the olefin metathesis reaction to polymer synthesis has established ring-opening metathesis polymerization and acyclic diene metathesis[2,6] as attractive, relatively new approaches to highly functionalized olefin-containing polymers. Finally, ring-closing metathesis,[11−14] including enantioselective variants,[12] and various cross-metathesis methodologies[15] are forefront in catalytic applications to the preparation of fine chemicals.

Once the Chauvin mechanism[16] for olefin metathesis was established,[17−21] the key discovery in the development of the process was the synthesis of stable metal alkylidene complexes, i.e., $L_nM{=}CRR'$ (R, R′ = H, aryl, ^{t}Bu, etc.), that served as catalysts or catalyst precursors. Schrock's seminal synthetic work, and the advent of α-abstraction as a synthetic tool,[21−23] enabled early transition metal chemistry to showcase olefin

[†] Cornell University.
[‡] University of North Texas.

(1) (a) Rouhi, A. M. *Chem. Eng. News* **2002**, *80*, 29−33. (b) Rouhi, A. M. *Chem. Eng. News* **2002**, *80*, 34−38.
(2) Grubbs, R. H., Ed. *Handbook of Metathesis*; Wiley & Sons: New York, 2003.
(3) Ivin, K. J.; Mol, J. C. *Olefin Metathesis and Metathesis Polymerization*; Academic Press: New York, 1997.
(4) Parshall, G. W.; Ittel, S. D. *Homogeneous Catalysis*; Wiley & Sons: New York, 1992.
(5) Mol, J. C. *J. Mol. Catal. A; Chem.* **2004**, *213*, 39−45.
(6) Buchmeiser, M. R. *Chem. Rev.* **2000**, *100*, 1565−1604.
(7) Fürstner, A. *Angew. Chem., Int. Ed.* **2000**, *39*, 3012−3043.
(8) Mol, J. C. *Green Chem.* **2002**, *4*, 5−13.
(9) Freitas, E. R.; Gum, C. R. *Chem. Eng. Prog.* **1979**, *75*, 73−76.
(10) Reuben, B.; Wittcoff, H. *J. Chem. Educ.* **1988**, *65*, 605−607.
(11) (a) Grubbs, R. H.; Chang, S. *Tetrahedron* **1998**, *54*, 4413−4450. (b) Grubbs, R. H.; Miller, S. J.; Fu, G. C. *Acc. Chem. Res.* **1995**, *28*, 446−552.
(12) (a) Schrock, R. R.; Hoveyda, A. H. *Angew. Chem., Int. Ed.* **2003**, *42*, 4592−4633. (b) Tsang, W. C. P.; Jernelius, J. A.; Cortez, G. A.; Weatherhead, G. S.; Schrock, R. R.; Hoveyda, A. H. *J. Am. Chem. Soc.* **2003**, *125*; 2591−2596. (c) Schrock, R. R.; Jamieson, J. Y.; Dolman, S. J.; Miller, S. A.; Bonitatebus, P. J., Jr.; Hoveyda, A. H. *Organometallics* **2002**, *21*, 409−417.
(13) Schuster, M.; Blechert, S. *Angew. Chem., Int. Ed. Engl.* **1997**, *36*, 2036−2056.
(14) Roy, R.; Das, S. K. *Chem. Commun.* **2000**, 519−529.
(15) (a) Chatterjee, A. K.; Choi, T. L.; Sanders, D. P.; Grubbs, R. H. *J. Am. Chem. Soc.* **2003**, *125*, 11360−11370. (b) Blackwell, H. E.; O'Leary, D. J.; Chatterjee, A. K.; Washenfelder, R. A.; Bussmann, D. A.; Grubbs, R. H. *J. Am. Chem. Soc.* **2000**, *122*, 58−71.
(16) Herrison, J. L.; Chauvin, Y. *Makromol. Chem.* **1970**, *141*, 161.
(17) Katz, T. J. *Adv. Organomet. Chem.* **1978**, *16*, 283−317.
(18) Calderon, N.; Lawrence, J. P.; Ofstead, E. A. *Adv. Organomet. Chem.* **1979**, *17*, 449−492.
(19) (a) Love, J. A.; Sanford, M. S.; Day, M. W.; Grubbs, R. H. *J. Am. Chem. Soc.* **2003**, *125*, 10103−10109. (b) Dias, E. L.; Nguyen, S. T.; Grubbs, R. H. *J. Am. Chem. Soc.* **1997**, *119*, 3887−3897.
(20) Adlhart, C.; Hinderling, C.; Baumann, H.; Chen, P. *J. Am. Chem. Soc.* **2000**, *122*, 8204−8214.
(21) Schrock, R. R. *J. Mol. Catal. A: Chem.* **2004**, *213*, 21−30.
(22) (a) Schrock, R. R. *Acc. Chem. Res.* **1979**, *12*, 98−104. (b) Schrock, R. R. *Pure Appl. Chem.* **1994**, *66*, 1447−1454. (c) Feldman, J.; Schrock, R. R. *Prog. Inorg. Chem.* **1991**, *39*, 1−74. (d) Schrock, R. R. *Acc. Chem. Res.* **1990**, *23*, 158−165.

metathesis in detailed mechanistic studies and catalytic applications. More recently, the dramatic increase in functionality tolerance exhibited by Grubbs' catalysts[2,11,15,19,24] and variants[7] and Schrock's creative exploitation of molybdenum[12,21] have exponentially increased the use of olefin metathesis in fine chemicals synthesis.[7,11−15]

Early in the history of alkylidene development, it was recognized that rearrangement of $L_nM{=}CR(CH_2R'')$ to an olefin complex $L_nM(RHC{=}CHR'')$ could be a potentially damaging process in relation to metathesis catalysis. In fact, the seeming inability to synthesize alkylidenes with β-CH bonds was often blamed on their intrinsic instability with respect to a bound olefin, i.e., $K_{alk/ole} < 1$ in eq 1.[25] While most studies regarding

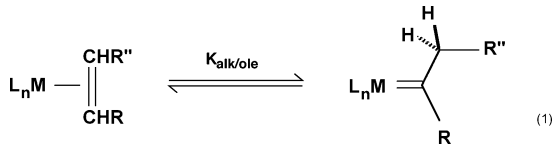

(1)

olefin metathesis appear to support this premise, a limited number of specific mechanistic studies have been attempted. An investigation of cationic rhenium complexes by Gladysz and Hatton led to an interpretation of the system ($K_{alk/ole} < 1$) as an organometallic Wagner−Meerwein rearrangement in reference to its carbocation-like hydrogen migration.[26] A study by Bercaw et al. of cyclometalated tantalum olefin and alkene complexes showed only a modest thermodynamic preference for the latter.[27] A significant number of observations suggest that a blanket statement pertaining to the instability of alkylidenes with β-hydrogens is dogmatic. Schrock et al. have catalyzed the rearrangement of ethylene to ethylidene via addition of $PhPH_2$,[28] and there are several other systems in which a greater thermodynamic stability of the alkylidene is implicated by certain reactivity sequences,[29−35] including clear examples of olefin to alkylidene and alkylidyne rearrangements by Caulton et al.[34]

While the portrayal of β-hydrogen-substituted alkylidenes as intrinsically unstable is compelling in view of the limited number of stable examples, $L_nM{=}CR(CH_2R'')$ species must be intermediates in a variety of catalytic applications,[1−24] and their potential to rearrange does not appear to be a major stumbling block to utilization. Several questions remain. First, are $L_nM{=}CR(CH_2R'')$ species thermodynamically unstable with respect to their olefin congeners or are $K_{alk/ole}$ dependent on metal or substrate? Second, are these rearrangements kinetically swift, or are there substantial impediments to the rearrangement process?

In examining the chemistry of $(silox)_3NbL$ (**1**-NbL, L = pyr, 4-pic,[33] PMe_3)[36−38] and $(silox)_3Ta$ (**2**)[39−44] over the years, a number of olefin complexes have been prepared, but until recently, none had been subjected to high temperature thermolysis. Preliminary indications with $(silox)_3Nb(ole)$ (**1**-ole, ole = 1-butene, cyclohexene) and $[(silox)_3Nb]_2(\eta\text{-}1,2;\eta\text{-}5,6\text{-}^cC_8H_6)$ indicated that $K_{alk/ole} > 1$ at elevated temperatures.[36] Moreover, little olefin metathesis activity was noted, despite ligands that would be typically expected to support such reactivity. Given these tantalizing examples, and the prospect that the sterics intrinsic to the $(silox)_3M$ (M = Nb, **1**; Ta, **2**) core would permit interrogation of the olefin to alkylidene rearrangement without interference from olefin metathesis, a systematic study of eq 1 was conducted, and it is reported herein.

Results

Synthesis of $(silox)_3Nb(olefin)$ Complexes. Two methods were used to prepare niobium olefin complexes. The most practical preparation of $(silox)_3Nb(ole)$ (**1**-ole, ole = olefin) involved Na/Hg reduction of $(silox)_3NbCl_2$ (**3**) in the presence of an excess of olefin, typically with THF as the solvent (eq 2).[36,37]

$$\underset{\mathbf{3}}{(silox)_3NbCl_2} + \text{olefin (excess)} \xrightarrow[\text{Na/Hg, } -2\text{ NaCl}]{\text{THF, 24 h}} \underset{\mathbf{1}\text{-ole (ole} = {}^cC_7H_{10},\ 25\%;\ {}^cC_6H_{10},\ 40\%)}{(silox)_3Nb(ole)} \quad (2)$$

$$\underset{\mathbf{1}\text{-4-pic}}{(silox)_3Nb(4\text{-pic})} + \text{olefin (excess)} \xrightarrow{\text{benzene}} \underset{\mathbf{1}\text{-ole (ole} = C_2H_4,\ C_2H_3Me\ (67\%);\ C_2H_3Et\ (81\%);\ cis\text{-MeCHCHMe}\ (40\%);\ H_2CCHC_6H_4\text{-}p\text{-X, X} = H\ (44\%),\ OMe\ (46\%),\ CF_3\ (46\%))}{(silox)_3Nb(ole) + 4\text{-picoline}} \quad (3)$$

Yields are modest (~40%), but the synthesis is direct as long as an excess of olefin can be used. An alternative methodology

(23) (a) Schrock, R. R. *Chem. Rev.* **2002**, *102*, 145−179. (b) Schrock, R. R. *J. Chem. Soc., Dalton Trans.* **2001**, 2541−2550. (c) Wallace, K. C.; Liu, A. H.; Dewan, J. C.; Schrock, R. R. *J. Am. Chem. Soc.* **1988**, *110*, 4964−4977.
(24) Trnka, T. M.; Grubbs, R. H. *Acc. Chem. Res.* **2001**, *34*, 18−29.
(25) (a) Collman, J. P.; Hegedus, L. S.; Norton, J. R.; Finke, R. G. *Principles and Applications of Organotransition Metal Chemistry*; University Science Books: Mill Valley, CA. (b) Mingos, D. M. P. In *Comprehensive Organometallic Chemistry*; Wilkinson, G., Stone, F. G. A., Abel, E. W., Eds.; Pergamon: New York, 1982; Vol. 3, Chapter 19.
(26) (a) Roger, C.; Bodner, G. S.; Hatton, W. G.; Gladysz, J. A. *Organometallics* **1991**, *10*, 3266−3274. (b) Hatton, W. G.; Gladysz, J. A. *J. Am. Chem. Soc.* **1983**, *105*, 6157−6158.
(27) Parkin, G.; Bunel, E.; Burger, B. J.; Trimmer, M. S.; Van Asselt, A.; Bercaw, J. E. *J. Mol. Catal.* **1987**, *41*, 21−39.
(28) Freundlich, J. S.; Schrock, R. R.; Davis, W. M. *J. Am. Chem. Soc.* **1996**, *118*, 3643−3655.
(29) Miller, G. A.; Cooper, N. J. *J. Am. Chem. Soc.* **1985**, *107*, 709−711.
(30) Hughes, R. P.; Maddock, S. M.; Rheingold, A. L.; Guzei, I. A. *Polyhedron* **1998**, *17*, 1037−1043.
(31) Giannini, L.; Guillemot, G.; Solari, E.; Floriani, C.; Re, N.; Chiesi-Villa, A.; Rizzoli, C. *J. Am. Chem. Soc.* **1999**, *121*, 2797−2807.
(32) (a) Schrock, R. R.; Seidel, S. W.; Mosch-Zanetti, N. C.; Shih, K.-Y.; O'Donoghue, M. B.; Davis, W. M.; Reiff, W. M. *J. Am. Chem. Soc.* **1997**, *119*, 11876−11893. (b) Schrock, R. R.; Seidel, S. W.; Mosch-Zanetti, N. C.; Dobbs, D. A.; Shih, K.-Y.; Davis, W. M. *Organometallics* **1997**, *16*, 5195−5208.
(33) (a) Kleckley, T. S.; Bennett, J. L.; Wolczanski, P. T.; Lobkovsky, E. B. *J. Am. Chem. Soc.* **1997**, *119*, 247−248. (b) Kleckley, T. S., Ph.D. Thesis, Cornell University, Ithaca, NY, 1998.
(34) (a) Ozerov, O. V.; Pink, M.; Watson, L. A.; Caulton, K. G. *J. Am. Chem. Soc.* **2004**, *126*, 6363−6378. (b) Ozerov, O. V.; Pink, M.; Watson, L. A.; Caulton, K. G. *J. Am. Chem. Soc.* **2004**, *126*, 2105−2113. (c) Ozerov, O. V.; Pink, M.; Watson, L. A.; Caulton, K. G. *J. Am. Chem. Soc.* **2003**, *125*, 9604−9605.
(35) (a) Carmona, E.; Paneque, M.; Poveda, M. L. *J. Chem Soc., Dalton Trans.* **2003**, 4022−4029. (b) Padilla-Martinez, I. I.; Poveda, M. L.; Carmona, E.; Monge, M. A.; Ruiz-Valero, C. *Organometallics* **2002**, *21*, 93−104.
(36) Veige, A. S.; Wolczanski, P. T.; Lobkovsky, E. B. *Angew. Chem., Int. Ed.* **2001**, *40*, 3629−3632.
(37) Veige, A. S.; Kleckley, T. S.; Chamberlin, R. L. M.; Neithamer, D. R.; Lee, C. E.; Wolczanski, P. T.; Lobkovsky, E. B.; Glassey, W. V. *J. Organomet. Chem.* **1999**, *591*, 194−203.
(38) (a) Veige, A. S.; Slaughter, L. M.; Lobkovsky, E. B.; Wolczanski, P. T.; Matsunaga, N.; Decker, S. A.; Cundari, T. R. *Inorg. Chem.* **2003**, *42*, 6204−6224. (b) Veige, A. S.; Slaughter, L. M.; Wolczanski, P. T.; Matsunaga, N.; Decker, S. A.; Cundari, T. R. *J. Am. Chem. Soc.* **2001**, *123*, 6419−6420.
(39) Chadeayne, A. R.; Wolczanski, P. T.; Lobkovsky, E. B. *Inorg. Chem.* **2004**, *43*, 3421−3432.
(40) Neithamer, D. R.; LaPointe, R. E.; Wheeler, R. A.; Richeson, D. S.; Van Duyne, G. D.; Wolczanski, P. T. *J. Am. Chem. Soc.* **1989**, *111*, 9056−9072.

involved treatment of (silox)$_3$Nb(η-N,C-4-pic) (**1**-4-pic, 4-pic = 4-picoline) with a slight excess of olefin ($\geq$10 equiv in the cases of cyclohexene and norbornene).[36] A directly related method was used previously in the synthesis of (silox)$_3$Nb(η-H_2CCHPh) (**1**-C_2H_3Ph) from (silox)$_3$Nb(η-N,C-NC_5H_5).[34,37] In cases where the olefin is bulky or otherwise coordinates poorly, the 4-picoline can be a competitive binder. For example, no indication of 4-picoline displacement was evidenced when **1**-4-pic was exposed to >1 equiv of *trans*-2-butene, but the addition of 5.0 equiv of *cis*-2-butene afforded (silox)$_3$Nb(η-*cis*-$C_2H_2Me_2$) (**1**-*c*-2-butene), although some **1**-4-pic remained (~7%, K(eq 3) $\approx$ 3.0). Alternatively, (silox)$_3$NbPMe$_3$ (**1**-PMe$_3$)[38] could be used as a source of "(silox)$_3$Nb" (**1**), but the expense of this reagent limited its application to a few olefin adducts, as eq 4 indicates.

$$\underset{\textbf{1}\text{-PMe}_3}{(\text{silox})_3\text{NbPMe}_3} + \text{olefin (excess)} \xrightarrow{\text{pentane}} \underset{\textbf{1}\text{-ole (ole} = H_2CCH^tBu,\ 90\%;\ ^cC_5H_8,\ 50\%)}{(\text{silox})_3\text{Nb(ole)}} + \text{PMe}_3 \quad (4)$$

Olefin isomerization proved not to be a problem in regard to monitoring the olefin to alkylidene transformation. Thermolysis of (silox)$_3$Nb(η-*cis*-$C_2H_2Me_2$) (**1**-*c*-$C_2H_2Me_2$) in benzene-d_6 afforded (silox)$_3$Nb(η-C_2H_3Et) (**1**-C_2H_3Et) after 3 d at 75 °C (eq 5),

$$\underset{\textbf{1}\text{-}c\text{-}C_2H_2Me_2}{(\text{silox})_3\text{Nb}(\eta\text{-}cis\text{-}C_2H_2Me_2)} \xrightarrow[75\ ^\circ\text{C, 3 d}]{C_6D_6} \underset{\textbf{1}\text{-}C_2H_3Et}{(\text{silox})_3\text{Nb}(\eta\text{-}C_2H_3Et)} \quad (5)$$

and the corresponding butene to butenylidene rearrangement required more severe conditions (vide infra). Furthermore, no evidence of disubstituted alkylidenes was observed, save those derived from cyclic olefins. The niobium olefin adducts were typically green, although the styrene derivatives tended toward brown. ^{1}H and ^{13}C{^{1}H} NMR spectral data on the olefin complexes are given in Supporting Information.

Synthesis of (silox)$_3$Ta(olefin) Complexes. Because of the availability of (silox)$_3$Ta (**2**),[40] the orange to red tantalum alkene adducts were simply prepared (some previously)[42] via the addition of excess olefin (e.g., ~1.1 equiv for styrene to ~30 equiv for cyclohexene) in various hydrocarbon solvents according to eq 6.

$$\underset{\textbf{2}}{(\text{silox})_3\text{Ta}} + \text{olefin (excess)} \rightarrow \underset{\begin{array}{c}\textbf{2}\text{-ole (ole} = C_2H_4\ (62\%);\ C_2H_3Me\ (56\%);\\ C_2H_3Et\ (67\%);\ ^cC_5H_8\ (63\%);\ ^cC_6H_{10}\ (55\%);\\ ^cC_7H_{10}\ (47\%);\ H_2C{=}CHC_6H_4\text{-}p\text{-X},\\ \text{X} = \text{H (65\%), OMe (62\%), CF}_3\ (76\%)\end{array}}{(\text{silox})_3\text{Ta(ole)}} \quad (6)$$

A large excess of hindered olefins was used to minimize competition from cyclometalation, which had been previously noted for slow *cis*-2-butene addition.[42] The reactions were rapid (<1 h) for all but norbornene, cyclopentene, and cyclohexene, which were allowed to react for 12−24 h.[45] Note that (silox)$_3$Ta(η-$C_2H_3{}^tBu$) (**2**-$C_2H_3{}^tBu$), the neohexene derivative, could not be cleanly synthesized, even when ~30 equiv of $H_2C{=}CH^tBu$ were present. Use of ~500 equiv $H_2C{=}CH^tBu$ afforded a substantial amount (>50%) of **2**-$C_2H_3{}^tBu$ after 24 h at 23 °C, but some alkylidene (silox)$_3$Ta=$CHCH_2{}^tBu$ (**2**=$CHCH_2{}^tBu$) had already formed, and additional species were present; hence the rearrangement of this olefin was not pursued further. Spectral data on the tantalum derivatives are also given in Supporting Information.

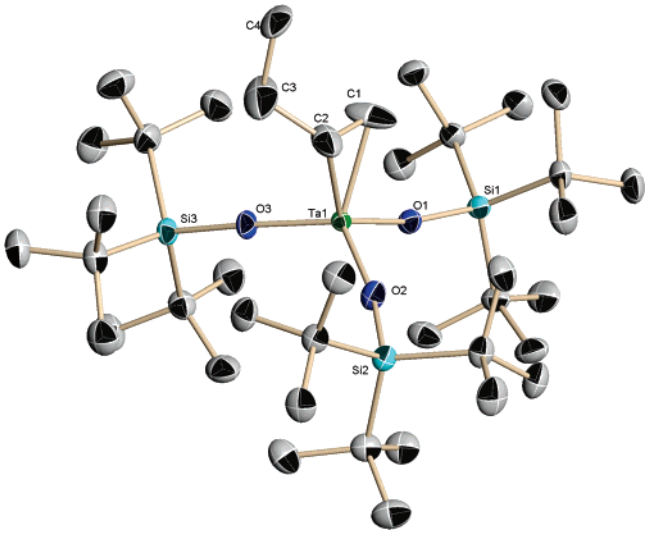

Figure 1. Molecular view of (silox)$_3$Ta(η-C_2H_3Et) (**2**-C_2H_3Et). Selected bond distances (Å) and angles (deg) not in text: C1−C2, 1.395(7); C2−C3, 1.494(7); C3−C4, 1.536(7); Si1−O, 1.664(2); Si2−O2, 1.678(3); Si3−O3, 1.685(2); O1−Ta−C1, 91.4(2); O2−Ta−C1, 116.0(2); O3−Ta−C1, 111.8(2); O1−Ta−C2, 128.7(2); O2−Ta−C2, 95.6(2); O3−Ta−C2, 100.0-(2); C1−Ta−C2, 37.9(2); C1−C2−Ta, 68.7(2); C2−C1−Ta, 73.3(3); C1−C2−C3, 115.2(6); C2−C3−C4, 113.9(4); Ta−O1−Si1, 165.63(14); Ta−O2−Si2, 167.89(15); Ta−O3−Si3, 172.81(16).

Structure of (silox)$_3$Ta(η-C_2H_3Et) (2-C_2H_3Et). As a typical asymmetric olefin complex, (silox)$_3$Ta(η-C_2H_3Et) (**2**-C_2H_3Et) was selected for structural examination, and data collection and refinement information may be found in Supporting Information. Figure 1 reveals the molecular structure of **2**-C_2H_3Et and gives pertinent bond distances and angles. The C1−C2 double bond has been lengthened to 1.395(7) Å, and the unit is oriented primarily along the Ta−O1 vector, but slightly skewed such that the Et group can best fit in the gap between the Si2 and Si3 silox ligands. Given the noted reducing power of the (silox)$_3$Ta (**2**) core, it is actually surprising that the C1−C2 lengthening is not greater;[46,47] perhaps the steric bulk of the silox groups is mitigating the potential back-donation of the Ta(III) d^2 metal center, or its unique electronic features[38,39] are

(41) Bonanno, J. B.; Henry, T. P.; Neithamer, D. R.; Wolczanski, P. T.; Lobkovsky, E. B. *J. Am. Chem. Soc.* **1996**, *118*, 5132−5133.
(42) Covert, K. J.; Neithamer, D. R.; Zonnevylle, M. C.; LaPointe, R. E.; Schaller, C. P.; Wolczanski, P. T. *Inorg. Chem.* **1991**, *30*, 2494−2508.
(43) Miller, R. L.; Toreki, R.; LaPointe, R. E.; Wolczanski, P. T.; Van Duyne, G. D.; Roe, D. C. *J. Am. Chem. Soc.* **1993**, *115*, 5570−5588.
(44) Wolczanski, P. T. *Polyhedron* **1995**, *14*, 3335−3362.
(45) Hirsekorn, K. F.; Wolczanski, P. T.; Cundari, T. R., manuscript in preparation.
(46) (a) Rietveld, M. H. P.; Teunissen, W.; Hagen, H.; van de Water, L.; Grove, D. M.; van der Schaaf, P. A.; Muhlebach, A.; Kooijman, H.; Smeets, W. J. J.; Veldman, N.; Spek, A. L.; van Koten, G. *Organometallics* **1997**, *16*, 1674−1684. (b) Abbenhuis, H. C. L.; Feiken, N.; Grove, D. M.; Jastrzebski, J. T. B. H.; Kooijman, H.; Vandersluis, P.; Smeets, W. J. J.; Spek, S. L.; van Koten, G. *J. Am. Chem. Soc.* **1992**, *114*, 9773−9781.
(47) (a) Schultz, A. S.; Brown, R. K.; Williams, J. M.; Schrock, R. R. *J. Am. Chem. Soc.* **1981**, *103*, 169−176. (b) Burger, B.; Santarsiero, B. D.; Trimmer, M. S.; Bercaw, J. E. *J. Am. Chem. Soc.* **1988**, *110*, 3134−3146. (c) Visciglio, V. M.; Nguyen, M. T.; Clark, J. R.; Fanwick, P. E.; Rothwell, I. P. *Polyhedron* **1996**, *15*, 551−554.

Scheme 1

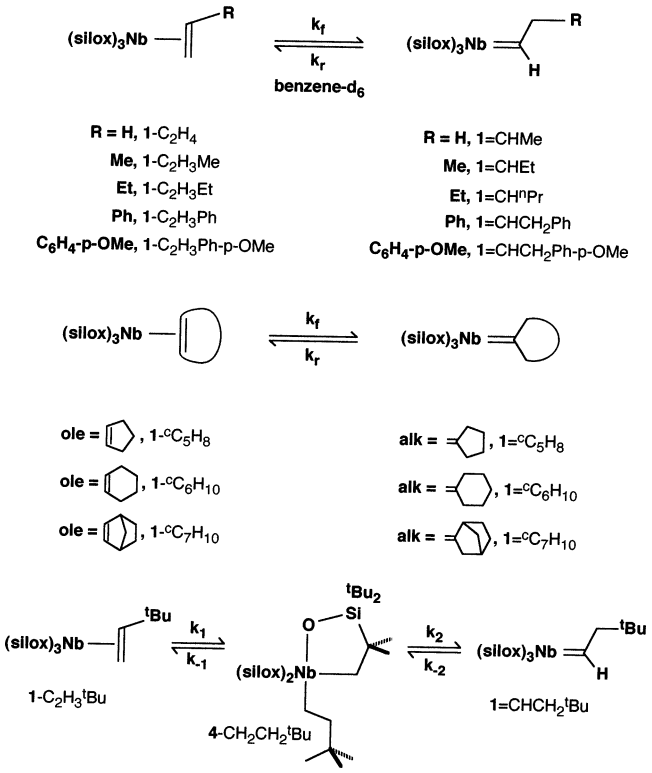

hampering binding. The d(Ta−O1) of 1.943(2) Å is longer than the remaining siloxide lengths (d(Ta−O2) = 1.907(2) Å, d(Ta−O3) = 1.892(2) Å) in response to the subtle influence of the 1-butene binding, and the O2−Ta−O3 angle has opened up (119.25(11)°) relative to O1−Ta−O2 (104.68(10)°) and O1−Ta−O3 (109.50(10)°) to accommodate the ethyl group. As expected, binding of the 1-butene is asymmetric with the β-carbon−tantalum distance ~0.06 Å longer than the α-carbon (2.174(4) vs 2.115(4) Å). The nearest silox−hydrogen to the β-carbon is 3.30 Å away, and its carbon is 4.05 Å distant.

Niobium Olefin to Alkylidene. 1. Observations. Thermolyses of the niobium olefin complexes (silox)$_3$Nb(ole) (ole = C_2H_4, **1**-C_2H_4; C_2H_3Me, **1**-C_2H_3Me; C_2H_3Et, **1**-C_2H_3Et;[36] $^cC_5H_8$, **1**-$^cC_5H_8$; $^cC_6H_{10}$, **1**-$^cC_6H_{10}$;[36] $^cC_7H_{10}$, **1**-$^cC_7H_{10}$; $H_2CCHC_6H_4$-*p*-X (X = H, **1**-C_2H_3Ph; OMe, **1**-C_2H_3Ph-*p*-OMe)) were undertaken at various temperatures. In these cases, smooth and reversible formation of the respective alkylidene complexes (silox)$_3$Nb(alk) (alk = CHMe, **1**=CHMe; CHEt, **1**=CHEt; CH^nPr, **1**=CH^nPr; $^cC_5H_8$, **1**=$^cC_5H_8$; $^cC_6H_{10}$, **1**=$^cC_6H_{10}$; $^cC_7H_{10}$, **1**=$^cC_7H_{10}$; $CHCH_2C_6H_4$-*p*-X (X = H, **1**=$CHCH_2$Ph; OMe, **1**=$CHCH_2$Ph-*p*-OMe)) was observed in benzene-d_6 according to Scheme 1. The compounds were assayed by ^{1}H and ^{13}C{^{1}H} NMR spectroscopy, but difficulties were encountered in observing the alkylidene carbons because of quadrupolar broadening by niobium. Heteronuclear quantum coherence methods permitted assessment of the chemical shifts of **1**=CHEt (δ 228) and **1**=CH^nPr (δ 249.0), while synthesis of (silox)$_3$Nb=$^{13}CH^{13}CH_3$ (**1**=$^{13}CH^{13}CH_3$, δ 213.0, J_{CH} = 114 Hz) allowed direct detection of its alkylidene resonance and evidence of a modest agostic interaction. Since J_{CH} for niobium alkylidenes cannot be easily observed, IR spectra were carefully scrutinized, but absorbances characteristic of agostic interactions were not noted.[23,48,49] NMR spectral data are given in Supporting Information.

For the case of nexohexene, a mechanistic clue was uncovered when another species was observed. Upon thermolysis at 103 °C for ~12 h, (silox)$_3$Nb(η-$C_2H_3{}^tBu$) (**1**-$C_2H_3{}^tBu$) was converted to the alkylidene (silox)$_3$Nb=$CHCH_2{}^tBu$ (**1**=$CHCH_2{}^tBu$, 25%), but another species tentatively formulated as the "tuck-in" neohexyl complex (silox)$_2$($^tBuCH_2CH_2$)Nb(κ^2-O,C-OSi^tBu_2-CMe_2CH_2) (**4**-$CH_2CH_2{}^tBu$, 25%) was also present. The disappearance of **1**-$C_2H_3{}^tBu$ corresponded roughly to the growth of **4**-$CH_2CH_2{}^tBu$, and initial rate studies provided a rate constant of $k \approx 3.6 \times 10^{-7}$ s^{-1} ($\Delta G^{\ddagger} \approx 33.3$ kcal/mol). Unfortunately, the severity of overlapping resonances hampered integration efforts to the point where simulation of the concentration vs time profiles of the three species that were obtained did not lead to convergence. In time, complete conversion to **1**=$CHCH_2{}^tBu$ was noted. It is tempting to conclude that a **1**-$C_2H_3{}^tBu$ ⇌ **4**-$CH_2CH_2{}^tBu$ ⇌ **1**=$CHCH_2{}^tBu$ sequence is operable, but the possibility that cyclometalation[50] is simply a side reaction cannot be discounted.

2. Kinetics and Thermodynamics. The data affiliated with each case are given in Table 1, along with pertinent activation parameters obtained from Eyring plots that typically were limited to a temperature range of ~40 °C because of the elevated temperatures required for reasonable rates. Aside from ethylene and styrene, no $K_{alk/ole}$ values were obtained because only the alkylidene was observed after a period of time. Since the thermolyses were conducted at relatively high temperatures, a common temperature was sought as a reference state at which the niobium and tantalum activation free energies could be compared. Although 103 °C was a rather low temperature for the observation of most niobium reactions, it was convenient for the equivalent, more elaborate tantalum processes, and therefore served as an appropriate reference condition.

For the cases listed in Table 1, no intermediates were detected, and the rate of olefin complex rearrangement is styrene ≈ ethylene < *para*-methoxystyrene < propene < 1-butene < cyclopentene < norbornene < cyclohexene. As the size of the olefin increases, and as more electron-donating substituents are present, the rate of rearrangement becomes faster. For the styrenes, the electron-withdrawing nature of the phenyl groups must compensate for the larger size of this olefin, rendering these cases quite slow. Note that having an electron donating substituent (OMe) in the para-position speeds up the rate of rearrangement relative to styrene, as expected.

In the niobium ethylene case, a van't Hoff plot corroborated the activation energies and revealed a large positive $\Delta S^{\circ} = 12.5$ (10) eu that helped compensate for a $\Delta H^{\circ} = 6.3$ (4) kcal/mol. With only one carbon bound to Nb, (silox)$_3$Nb=CHMe (**1**=CHMe) is less constrained in both the alkylidene (e.g., methyl rotor, etc.) and siloxide periphery, rendering it entropically more favorable than the parent ethylene species, (silox)$_3$Nb(η^2-C_2H_4) (**1**-C_2H_4). It is suspected that the alkylidene is more favored entropically in all cases, although perhaps less so for the cyclic derivatives.

3. Attempts at α-Substituent Effects. In an attempt at further electronic substituent studies, the 170 °C thermolysis of

(48) Brookhart, M.; Green, M. L. H.; Wong, L. *Prog. Inorg. Chem.* **1988**, *36*, 1−124.
(49) Goddard, R. J.; Hoffmann, R.; Jemmis, E. D. *J. Am. Chem. Soc.* **1980**, *102*, 7667−7676.
(50) (a) Rothwell, I. P. *Acc. Chem. Res.* **1988**, *21*, 153−159. (b) Rothwell, I. P. *Polyhedron* **1985**, *4*, 177−200.

Table 1. Rate Constants[a] (k_f (Scheme 1) unless Noted)[b] and Activation Parameters for the (silox)$_3$Nb(ol) (**1**-ol) ⇌ (silox)$_3$Nb(alk) (**1**═alk) Rearrangement ($\Delta G°$, $\Delta G^‡$, and $\Delta H^‡$ in kcal/mol; $\Delta S^‡$ in eu) and Related Processes

reaction	T (°C)[c]	k ($\times 10^5$ s^{-1})	$\Delta G_f^‡$	$G_{103°C}^‡$	$\Delta H^‡$	$\Delta S^‡$	$\Delta G_{103°C}°$
1-C_2H_4 ⇌ **1**═CHMe	155	0.371(1)		35.5(3)	31.9(3)	−9.6(2)	1.60(44)[d]
		1.22(2)[b]		33.3(8)[b]	24.7(6)[b]	−22.8(14)[b]	2.2(10)[e]
	168	1.14(2)					
		2.75(5)[b]					
	180	3.20(6)					
		6.88(8)[b]					
	196	10.63(1)					
		17.54(4)[b]					
1-C_2H_3Me ⇌ **1**═CHEt	140	1.63(2)		33.4(41)	29.6(40)	−10.1(25)	
	155	3.54(2)					
	166	10.3(3)					
	180	42.2(19)					
1-C_2H_3Et ⇌ **1**═CH^{n}Pr	150	6.44(6)		32.7(2)	28.3(2)	−11.6(3)	
	166	22.7(5)					
		22.9(3)[f]	33.3(1)[f]				
	182	72.0(16)					
	190	130(1)					
1-D_2CCHEt → **1**═CD^{n}Pr-d_2	166[f]	9.24(7)[f]	34.1(1)[f]				
1-$C_2H_3{}^t$Bu → **4**-$CH_2CH_2{}^t$Bu	103	0.036[g]	33.3[g]				
1-$^cC_5H_8$ ⇌ **1**═C$(CH_2)_3CH_2$	103	0.385(6)		31.50(6)			
1-$^cC_7H_{10}$ ⇌ **1**═$^cC_7H_{10}$	103	0.765(11)		30.98(6)			
		0.00404[h]		34.9[h]			
	166	111(6)[i]	32.0(1)[i]				
		0.617(17)[h]	36.5(1)[h]				
1-$^cC_7H_8D_2$ ⇌ **1**═$^cC_7H_9$D-d_2	166	49.8(8)[i]	32.7(1)[i]				
1-$^cC_6H_{10}$ ⇌ **1**═ $^cC_6H_{10}$	60	0.0787(8)		29.5(2)	23.8(2)	−15.2(3)	
	70	0.225(4)					
	86	1.18(3)					
	103	5.38(17)					
1-−C_2H_3Ph ⇌ **1**═CHCH$_2$Ph	155	0.321(2)	36.11(3)	*35.5* (est)[j]			0.6[k]
		0.325(5)[b]	36.11(6)	*34.9* (est)[b,l]			*0.6* (est)[e,l]
1-C_2H_3Ph-*p*-OMe ⇌ **1**═CHCH$_2$Ph-*p*-OMe	155	0.566(4)	35.63(4)	*35.0* (est)[j]			0.2[k]
		0.337(10)[b]	36.1(1)	*34.8* (est)[b,l]			*0.2* (est)[e,l]

[a] Rate constants were obtained from first-order loss of **1**-ole, approach to equilibrium kinetics, or from simulation of the latter as necessary and are the average of three simultaneous kinetics runs. [b] Rate constants and parameters corresponding to k_r. [c] Temperatures are estimated to be ±0.5 °C. [d] From van't Hoff plot of direct measurements of $K_{alk/ol}$ at the temperatures indicated: $\Delta H° = 6.30(44)$ kcal/mol and $\Delta S° = 12.5(10)$ eu. [e] Taken from $\Delta G_f^‡ - \Delta G_r^‡$. [f] Conducted in tandem (triplicate tubes for each) to afford $k_H/k_D = z_f = 2.5$ at 166 °C. [g] Rough rate constant obtained from initial rates on the disappearance of **1**-$C_2H_3{}^t$Bu. [h] Rate constant for k_r as determined from KIE experiments at 166 °C as described in text. The $\Delta G_r^‡$ at 103 °C was obtained by assuming $\Delta S° \approx 12$ eu. [i] Conducted in tandem (triplicate tubes for each) to afford $k_H/k_D = z_f = 2.3$ at 166 °C. [j] Estimated using $\Delta S^‡ = -12$ eu, a reasonable average of similar activation entropies. [k] $K_{alk/ol}$ measured directly at 155 °C and corrected to 103 °C using $\Delta S° \approx 13$ from the ethylene case. [l] Estimated using $\Delta S^‡ \approx -24$ eu obtained from an estimate of −12 eu for the forward step and $\Delta S° \approx 12$ eu from the ethylene case.

(silox)$_3$Nb(η-$C_2H_3C_6H_4$-*p*-CF_3) (**1**-C_2H_3Ph-*p*-CF_3) was undertaken, but CF bond activation[51−55] was noted instead of the expected alkylidene. To examine the potential for Fischer-type carbenes to rearrange, (silox)$_3$NbPMe$_3$ (**1**-PMe$_3$) was exposed to methylvinyl ether and vinylfluoride, respectively. It was hoped that (silox)$_3$Nb(η-C_2H_3X) (X = OMe, **1**-C_2H_3OMe; F, **1**-C_2H_3F) would form and be converted to (silox)$_3$Nb═CXCH$_3$ or (silox)$_3$-Nb═CHCH$_2$X over time, but NMR tube experiments indicated that C−X bond activation occurred to give (silox)$_3$(H$_2$C═CH)-NbX (X = OMe, **5**-OMe; F, **5**-F) (eq 7).

$$\underset{\textbf{1}\text{-PMe}_3}{(\text{silox})_3\text{NbPMe}_3} + \text{H}_2\text{C}{=}\text{CHX} \xrightarrow[23\ °\text{C}]{\text{benzene-}d_6} (\text{silox})_3(\text{H}_2\text{C}{=}\text{CH})\text{NbX} + \text{PMe}_3 \quad (7)$$
$$\text{X} = \text{OMe}, \textbf{5}\text{-OMe}; \text{F}, \textbf{5}\text{-F}$$

Given the precedent set by the oxidative addition of 2,3-dihydrofuran to (silox)$_3$Ta (**2**),[56] these results were anticipated, but it was nonetheless disappointing that formation of Fischer carbenes seemed untenable.

Structure of (silox)$_3$Nb═^{c}C$_6$H$_{10}$ (1═^{c}C$_6$H$_{10}$). The niobium cyclohexylidene complex, (silox)$_3$Nb═^{c}C$_6$H$_{10}$ (**1**═^{c}C$_6$H$_{10}$), was chosen for further structural characterization (see Supporting Information for crystallographic details). One of four crystallographically distinct molecules of **1**═^{c}C$_6$H$_{10}$ is shown in Figure 2, and some average bond distances and angles are also listed. The average d(Nb═C) is 1.956(18) Å, which is typical for a niobium alkylidene.[22,23,36,57,58] While no significant deviations in average Nb−O bond distances (1.917(28) Å) are observed, one O−Nb−O angle (125.3(15)° ave) was substantially wider than the remaining O−Nb−O angles of 107.7(13)° (ave), despite similar O−Nb−C angles (105.1(21)° ave). The NbC$(C_\alpha)_2$ plane is nearly perpendicular to one Nb−O bond, and the chair of

(51) (a) Clot, E.; Megret, C.; Kraft, B. M.; Eisenstein, O.; Jones, W. D. *J. Am. Chem. Soc.* **2004**, *126*, 5647−5653. (b) Jones, W. D. *J. Chem. Soc., Dalton Trans.* **2003**, 3991−3995.
(52) Strazisar, S. A.; Wolczanski, P. T. *J. Am. Chem. Soc.* **2001**, *123*, 4728−4740.
(53) Watson, L. A.; Yandulov, D. V.; Caulton, K. G. *J. Am. Chem. Soc.* **2001**, *123*, 603−611.
(54) Edelbach, B. L.; Jones, W. D. *J. Am. Chem. Soc.* **1997**, *119*, 7734−7742.
(55) (a) Ferrando-Miguel, G.; Gerard, H.; Eisenstein, O.; Caulton, K. G. *Inorg. Chem.* **2002**, *41*, 644−6449. (b) Huang, D. J.; Koren, P. R.; Folting, K.; Davidson, E. R.; Caulton, K. G. *J. Am. Chem. Soc.* **2000**, *122*, 8916−8931.
(56) Bonanno, J. B.; Henry, T. P.; Neithamer, D. R.; Wolczanski, P. T.; Lobkovsky, E. B. *J. Am. Chem. Soc.* **1996**, *118*, 5132−5133.
(57) Caselli, A.; Solari, E.; Scopelliti, R.; Floriani, C. *J. Am. Chem. Soc.* **1999**, *121*, 8296−8305.
(58) Nugent, W. A.; Mayer, J. M. *Metal−Ligand Multiple Bonds*; Wiley-Interscience: New York, 1988.

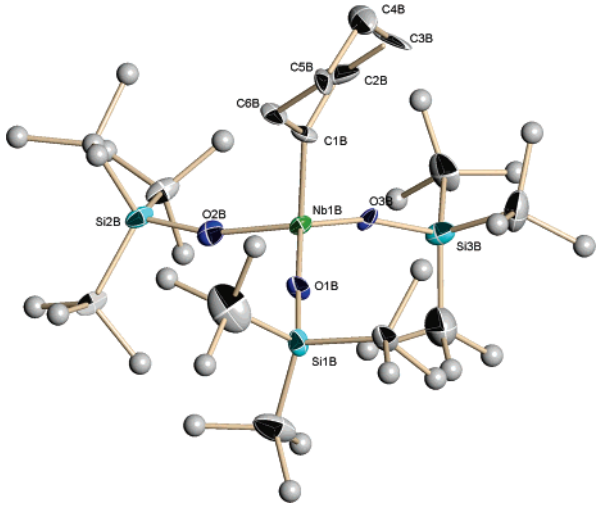

Figure 2. Molecular view of one of the four crystallographically distinct molecules of (silox)$_3$Nb=^{c}C$_6$H$_{10}$ (**1**=^{c}C$_6$H$_{10}$). Selected bond distances (Å) and angles (deg) not in text: Si−O(ave), 1.660(28); C−C(ring ave), 1.519(47); Nb−C−C(ave), 124.5(15); C−C−C(ring ave), 110.9(22); Nb−O−Si(ave), 169.8(65).

the cyclohexane ring is disposed toward the unique, wide O−Nb−O angle, which presumably reflects its steric influence. The closest silox−hydrogen to the alkylidene carbon is a mere 3.06 Å away, and its carbon is 4.00 Å distant.

Tantalum Olefin to Alkylidene. 1. Observations. Thermolyses of the tantalum olefin complexes (silox)$_3$Ta(ole) (ole = C_2H_4, **2**-C_2H_4; C_2H_3Me, **2**-C_2H_3Me; C_2H_3Et, **2**-C_2H_3Et; $^cC_5H_8$, **2**-$^cC_5H_8$; $^cC_6H_{10}$, **2**-$^cC_6H_{10}$; $H_2CCHC_6H_4$-*p*-X (X = H, **2**-C_2H_3Ph; OMe, **2**-C_2H_3Ph-*p*-OMe; CF_3, **2**-C_2H_3Ph-*p*-CF_3)) were undertaken at temperatures somewhat lower than those of the niobium study. As Scheme 2 reveals, typically two species were observed: the "tuck-in" alkyls (silox)$_2$(R)Ta(κ^2-O,C-OSi^{t}Bu$_2$CMe$_2$CH$_2$) (**6**-R: R = Et, **6**-Et; ^{n}Pr, **6**-^{n}Pr; ^{n}Bu, **6**-^{n}Bu; ^{c}Pe, **6**-^{c}Pe; ^{c}Hex, **6**-^{c}Hex; $CH_2CH_2C_6H_4$-*p*-X (X = H, **6**-CH_2CH_2Ph; OMe, **6**-CH_2CH_2Ph-*p*-OMe; F, **6**-CH_2CH_2-Ph-*p*-F)), and the alkylidenes (silox)$_3$Ta(alk) (alk = CHMe, **2**=CHMe; CHEt, **2**=CHEt; CH^{n}Pr, **2**=CH^{n}Pr; $^cC_5H_8$, **2**=$^cC_5H_8$; $^cC_6H_{10}$, **2**=$^cC_6H_{10}$; $CHCH_2C_6H_4$-*p*-X (X = H, **2**=$CHCH_2Ph$; OMe, **2**=$CHCH_2Ph$-*p*-OMe; F, **2**=$CHCH_2Ph$-*p*-F)). Only the norbornene derivative, (silox)$_3$Ta(η-^{c}C$_7$H$_{10}$) (**2**-^{c}C$_7$H$_{10}$), smoothly converted to the norbornylidene (silox)$_3$Ta=^{c}C$_7$H$_{10}$ (**2**=^{c}C$_7$H$_{10}$) without observation of the "tuck-in" alkyl (silox)$_2$(2-norbornyl)Ta(κ^2-O,C-OSi^{t}Bu$_2$CMe$_2$CH$_2$) (**6**-^{c}C$_7$H$_{11}$). For the tantalum alkylidenes, ^{13}C resonances of the alkylidenes were easily obtained, and their average chemical shift was 228.5(33) ppm, with exceptions being **2**=CHMe (δ 204.71, J_{CH} = 111 Hz) and **2**=CH^{n}Pr (δ 254.84, J_{CH} = 108 Hz); again, only modest agostic interactions were evident.[23,48,49]

2. Simulations and Assessment. Table 2 lists the cases studied and reveals the first-order rate constants assigned to the steps in Scheme 2. In many cases—ethylene, cyclopentene, and the styrenes—all three species could be observed throughout the course of reaction, but in some—propene, 1-butene, and cyclohexene—the intermediate "tuck-in" alkyls (**6**-R) and alkylidenes (**2**=alk) proved to be sufficiently stable relative to the starting olefin complexes that no **2**-ole was observable at equilibrium. Simulation of the concentration vs time profiles obtained via ^{1}H NMR spectra was required to determine all possible rate constants in each case.

Scheme 2

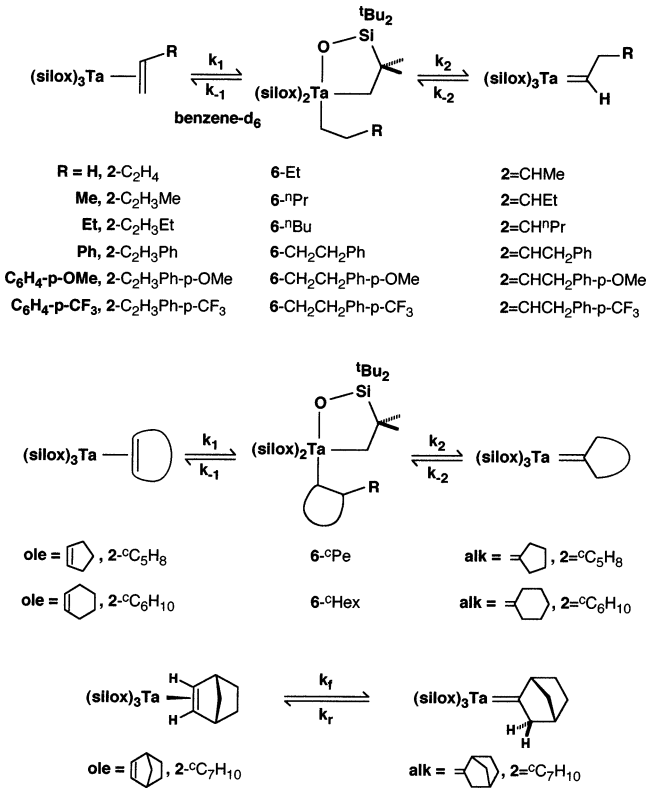

Rate constants coupled to species of low concentration were intrinsically less precise and probably less accurate, simply because of the quality of integration. Entropy of activation values, critical for estimating $\Delta G^{\ddagger}$'s at 103 °C in many cases, was estimated using the most accurate rate and thermodynamic (e.g., $\Delta S°$) data available. The following $\Delta S^{\ddagger}$ values were deemed reasonable estimates for several cases: $\Delta S_1^{\ddagger} \approx -10$ eu, $\Delta S_{-1}^{\ddagger} \approx \Delta S_2^{\ddagger} \approx -7$ eu, and $\Delta S_{-2}^{\ddagger} \approx -27$ eu. With the aid of $\Delta S°$ values determined from equilibrium measurements, the styrene $\Delta G_{103°C}^{\ddagger}$ values were estimated somewhat differently, with $\Delta S_1^{\ddagger} \approx -8$ eu, $\Delta S_{-1}^{\ddagger} \approx -14$ eu, $\Delta S_2^{\ddagger} \approx -8$ eu, and $\Delta S_{-2}^{\ddagger} \approx -27$ eu. Details are provided as Supporting Information.

As a partial check of the $\Delta S^{\ddagger}$ estimates, the temperature dependence of the rate of butene complex conversion to its "tuck-in" butyl, (silox)$_3$Ta(η-C_2H_3Et) (**2**-C_2H_3Et) → (silox)$_2$-(^{n}PrCH$_2$)Ta(κ^2-O,C-OSi^{t}Bu$_2$CMe$_2$CH$_2$) (**6**-^{n}Bu), was measured from 78 to 120 °C. The Eyring plot yielded activation parameters of $\Delta H_1^{\ddagger} = 24.8(1)$ kcal/mol and $\Delta S^{\ddagger} = -11(1)$ eu, in support of the above estimates. Note that the entropy of activation is similar to that found for the cyclometalation of (silox)$_3$Ta (**2**) to (silox)$_2$HTa(κ^2-O,C-OSi^{t}Bu$_2$CMe$_2$CH$_2$) (**8**, eq 8).

$$\underset{\mathbf{2}}{(\text{silox})_3\text{Ta}} \xrightarrow{\text{benzene-}d_6} \underset{\mathbf{8}}{(\text{silox})_2\text{HTa}(\kappa^2\text{-O,C-OSi}^t\text{Bu}_2\text{CMe}_2\text{CH}_2)} \quad (8)$$

The temperature dependence of this process yielded a $\Delta H^{\ddagger}$ of 19.9(27) kcal/mol and $\Delta S^{\ddagger}$ of −15(4) eu over a 52−104 °C range.[42]

3. Kinetics and Thermodynamics. Since the rate constants for all steps in Scheme 2 can be measured or estimated, a thermodynamic assessment of the rearrangement can be made. The alkylidene complexes are favored over the olefins in all

Table 2. Rate Constants ($\times 10^4$ s^{-1})[a] and Activation Free Energies ($\Delta G^{\ddagger}$ in kcal/mol) for the (silox)$_3$Ta(ol) (**2**-ol) $\rightleftharpoons$ (silox)$_2$(R)Ta(κ^2-O,C-OSi^{t}Bu$_2$CMe$_2$CH$_2$) (**6**-R) $\rightleftharpoons$ (silox)$_3$Ta(alk) (**2**=alk) Rearrangement (Scheme 2)

reaction	T (°C)[b]	k_1	k_{-1}	k_2	k_{-2}	$\Delta G_{103°C}^{\ddagger}(k_1)$	$\Delta G_{103°C}^{\ddagger}(k_{-1})$	$\Delta G_{103°C}^{\ddagger}(k_2)$	$\Delta G_{103°C}^{\ddagger}(k_{-2})$
2-C_2H_4 $\rightleftharpoons$ **6**-Et $\rightleftharpoons$ **2**=CHMe	130.5	15.3(4)	5.90(8)	0.177(11)	1.90(21)	28.4(39)[c]	29.3(23)[c]	31.9(27)[c]	29.5(35)[c,d]
	140.5	26.9(3)[e]	10.97(9)[e]	0.472(7)[e]	3.67(5)[e]				
	150	33.4(19)	14.2(8)	0.683(33)	3.91(24)	29.1(3)[f]	30.0(3)[f]	32.7(3)[f]	30.2(3)[f]
	170.5	146(12)	68.5(50)	2.70(14)	9.90(12)				
2-C_2H_3Me $\rightarrow$ **6**-^{n}Pr $\rightleftharpoons$ **2**=CHEt	103	1.304(7)				28.9(1)		32.5[g]	30.4[g]
	155			1.45(2)	5.07(20)				
2-C_2H_3Et $\rightarrow$ **6**-^{n}Bu $\rightleftharpoons$ **2**=CH^{n}Pr	78	0.103(8)[h]							
	93	0.432(4)[h]							
	103	1.42(4)[h]				28.8(1)		32.6[i]	30.6[i]
	120	4.87(5)[h]							
	155			1.19(3)	3.88(4)				
2-C_2H_3Et $\rightarrow$ **6**-^{n}Bu[j]	103	1.40(6)[j]				28.8(1)[j]			
2-D_2CCHEt $\rightarrow$ **6**-$CD_2{}^n$Pr[j]	103	0.924(7)[j]				29.1(1)[j]			
6-^{n}Bu $\rightleftharpoons$ **2**=CH^{n}Pr[k,l]	166			3.38(8)[k]				*32*.6[m]	
6-$CD_2{}^n$Pr $\rightarrow$ **2**=CD^{n}Pr-d_2[k]	166			0.547(6)[k]				34.2[n]	
6-CHD^{n}Pr $\rightarrow$ **2**=CH^{n}Pr-d_2[l]	166			0.387(10)[l]				34.5°	
2-^{c}C$_5$H$_8$ $\rightleftharpoons$ **6**-^{c}Pe $\rightleftharpoons$ **2**=C(CH$_2$)$_3$CH$_2$	103	2.97(5)	2.16(6)	3.77(12)	1.01(3)	28.2(2)	28.5(2)	28.1(9)	29.1(9)
2-^{c}C$_7$H$_{10}$ $\rightleftharpoons$ **2**=^{c}C$_7$H$_{10}$	103	0.584(5)[p]				29.5(1)[p]			
		0.0589(46)[q]					31.2(2)[q]		
2-^{c}C$_6$H$_{10}$ $\rightarrow$ **6**-^{c}Hex $\rightleftharpoons$ **2**=^{c}C$_6$H$_{10}$	103	5.54(6)		4.14(16)	1.90(9)	27.8(1)		28.0(1)	28.6(1)
2-C_2H_3Ph $\rightleftharpoons$ **6**-CH_2CH_2Ph $\rightleftharpoons$ **2**=CHCH$_2$Ph[s]	140	0.267(14)	0.0183(9)	0.0820(24)	0.350(28)	32.9(7)[r]	35.4(43)[r]	34.5(20)[r]	32.6(17)[r]
	155	1.02(2)[t]	0.178(5)[t]	0.57(2)[t]	1.92(7)[t]				
	166	2.31(4)	0.377(11)	1.40(3)	4.08(9)	32.8(1)[u,v]	33.9(8)[u,v]	33.3(4)[u,v]	31.3(4)[u,v]
	180	7.62(27)	1.28(5)	6.97(5)	13.1(10)				
2-C_2H_3Ph-*p*-OMe $\rightleftharpoons$ **6**-CH_2CH_2Ph-*p*-OMe $\rightleftharpoons$ **2**=CHCH$_2$Ph-*p*-OMe	155	1.83(2)	0.191(7)	0.70(4)	2.48(9)	32.3[u,w]	33.9[u,w]	33.1[u,w]	31.0[u,w]
2-C_2H_3Ph-*p*-CF_3 $\rightleftharpoons$ **6**-CH_2CH_2Ph-*p*-CF_3 $\rightleftharpoons$ **2**=CHCH$_2$Ph-*p*-CF_3	155	0.256(4)	0.136(2)	0.336(6)	0.984(6)	33.9[u,x]	34.2[u,x]	33.7[u,x]	31.8[u,x]
(silox)$_3$Ta (**2**) $\rightarrow$	52	0.572(6)[y]							
(silox)$_2$HTa(OSi^{t}Bu$_2$CMe$_2$CH$_2$) (**8**)	56	1.0(1)[z]							
	64	2.1(1)[z]							
	71	4.17(4)[y]							
	75	4.8(1)[z]							
	84	11.9(2)[y]							
	104	49.9(13)[y]				26.1(1)			

[a] Rate constants were obtained from simulation of the concentration vs T profile of the three species and are the average of three simultaneous kinetics runs unless otherwise noted; $\Delta G^{\ddagger}$'s were obtained directly from k's at 103 °C or from Eyring plots or estimates as noted. [b] Temperatures are estimated to be ±0.5 °C. [c] Activation free energies determined from Eyring plots ($\Delta H^{\ddagger}$ in kcal/mol, $\Delta S^{\ddagger}$ in eu): $\Delta H_1{}^{\ddagger} = 18.9(27)$, $\Delta S_1{}^{\ddagger} = -25.3(73)$; $\Delta H_{-1}{}^{\ddagger} = 20.7(1)$, $\Delta S_{-1}{}^{\ddagger} = -22.9(60)$; $\Delta H_2{}^{\ddagger} = 22.6(19)$, $\Delta S_2{}^{\ddagger} = -25(5)$; $\Delta H_{-2}{}^{\ddagger} = 13(2)$, $\Delta S_{-2}{}^{\ddagger} = -43(57)$. [d] The error in $\Delta S_{-2}{}^{\ddagger}$ was so great that this value was determined from measurement of $K(2)$ and thus $\Delta G°(2)$ ($\Delta G_{-2}{}^{\ddagger} = \Delta G°(2) - \Delta G_2{}^{\ddagger}$). From van't Hoff plot of $K(1) = k_1/k_{-1}$: $\Delta H°(1) = -1.7(1)$ kcal/mol, $\Delta S°(1) = -2.4(1)$ eu. From van't Hoff plot of $K(2) = k_2/k_{-2}$: $\Delta H°(2) = 9.5(6)$ kcal/mol, $\Delta S°(2) = 19.0(14)$ eu. [e] Taken from the average of two simultaneous kinetics runs. [f] Estimated from the 130.5 − 170.5 °C data using $\Delta S_1{}^{\ddagger} \approx -10$ eu, $\Delta S_{-1}{}^{\ddagger} \approx \Delta S_2{}^{\ddagger} \approx -7$ eu, and $\Delta S_{-2}{}^{\ddagger} = -27$ eu; the $\Delta G_{103°C}{}^{\ddagger}$'s for each step were calculated from each temperature and averaged. [g] Estimated from the 155 °C data ($\Delta G_2{}^{\ddagger} = 32.9(1)$ and $\Delta G_{-2}{}^{\ddagger} = 31.8(1)$ kcal/mol) using $\Delta S_2{}^{\ddagger} \approx -7$ eu and $\Delta S_{-2}{}^{\ddagger} \approx -27$ eu. [h] From an Eyring plot, the activation parameters for k_1 are $\Delta H_1{}^{\ddagger} = 24.8$ (1) and $\Delta S_1{}^{\ddagger} = -11(1)$. [i] Estimated from the 155 °C data ($\Delta G_2{}^{\ddagger} = 33.0(1)$ and $\Delta G_{-2}{}^{\ddagger} = 32.0(1)$ kcal/mol) using $\Delta S_2{}^{\ddagger} \approx -7$ eu and $\Delta S_{-2}{}^{\ddagger} \approx -27$ eu. [j] From a tandem measurement, $1.52 = z_1{}'^2 = (1.23)^2$ as in Scheme 4. [k] From fits of the approach to equilibria via tandem measurements, $z_2 z_2{}' = 6.2$ as in Scheme 4. [l] From fits of the approach to equilibria via tandem measurements, $z_2 = 4.4$ as in Scheme 4. By difference with the previous case, $z_2{}' = 1.4$. [m] Calculated from $\Delta G_{166°C}{}^{\ddagger} = 33.0(1)$ assuming $\Delta S_2{}^{\ddagger} = -7$ eu. [n] Calculated from $\Delta G_{166°C}{}^{\ddagger} = 34.6(1)$ assuming $\Delta S_2{}^{\ddagger} = -7$ eu. [o] Calculated from $\Delta G_{166°C}{}^{\ddagger} = 34.9(1)$ assuming $\Delta S_2{}^{\ddagger} = -7$ eu. [p] Corresponds to k_f of Scheme 2. [q] Corresponds to k_r of Scheme 2. [r] Activation free energies determined from Eyring plots ($\Delta H^{\ddagger}$ in kcal/mol, $\Delta S^{\ddagger}$ in eu): $\Delta H^{\ddagger}(k_1) = 30.0(7)$, $\Delta S^{\ddagger}(k_1) = -7.5(3)$; $\Delta H^{\ddagger}(k_{-1}) = 37.9(43)$, $\Delta S^{\ddagger}(k_{-1}) = 6.64(12)$; $\Delta H^{\ddagger}(k_2)^{\ddagger} = 39.7(20)$, $\Delta S^{\ddagger}(k_2) = 13.8(10)$; $\Delta H^{\ddagger}(k_{-2}) = 31.7(17)$, $\Delta S^{\ddagger}(k_{-2}) = -2.5(2)$. [s] From van't Hoff plots using $K(1)_{140°C} = 5.10$, $K(1)_{155°C} = 5.41$, $K(1)_{166°C} = 5.58$, $K(1)_{180°C} = 5.90$, $K(2)_{140°C} = 0.19$, $K(2)_{155°C} = 0.27$, $K(2)_{166°C} = 0.34$, and $K(2)_{180°C} = 0.51$: $\Delta H°(1) = 1.33(10)$ kcal/mol, $\Delta S°(1) = 6.46(22)$ eu, $\Delta H°(2) = 9.05(24)$ kcal/mol, $\Delta S°(2) = 18.56(38)$ eu. [t] At 155 °C (kcal/mol): $\Delta G_1{}^{\ddagger} = 33.2(1)$, $\Delta G_{-1}{}^{\ddagger} = 34.7$, $\Delta G_2{}^{\ddagger} = 33.7$, $\Delta G_{-2}{}^{\ddagger} = 32.6$. [u] Estimated from the 140−180 °C data using $\Delta S_1{}^{\ddagger} \approx -8$ eu, $\Delta S_{-1}{}^{\ddagger} \approx -14$ eu, $\Delta S_2{}^{\ddagger} = -8$ eu, and $\Delta S_{-2}{}^{\ddagger} = -27$ eu. [v] The $\Delta G_{103°C}{}^{\ddagger}$'s for each step were calculated at each temperature and averaged. [w] At 155 °C (kcal/mol): $\Delta G_1{}^{\ddagger} = 32.7(1)$, $\Delta G_{-1}{}^{\ddagger} = 34.6(1)$, $\Delta G_2{}^{\ddagger} = 33.5(1)$, $\Delta G_{-2}{}^{\ddagger} = 32.4(1)$. [x] At 155 °C (kcal/mol): $\Delta G_1{}^{\ddagger} = 34.4(1)$, $\Delta G_{-1}{}^{\ddagger} = 34.9(1)$, $\Delta G_2{}^{\ddagger} = 34.1(1)$, $\Delta G_{-2}{}^{\ddagger} = 33.2(1)$. [y] Rate constants for cyclometalation were determined by ^{1}H NMR spectroscopy. [z] Rate constants were determined from UV−vis spectroscopy according to ref 42. From an Eyring plot of all rate constants, the cyclometalation of **2** to **8** affords $\Delta H^{\ddagger} = 19.9(27)$ kcal/mol and $\Delta S^{\ddagger} = -15(4)$ eu; at 103 °C, $\Delta G^{\ddagger} = 25.5(30)$.

cases except ethylene and the styrenes, just as in the niobium system. However, the tuck-in alkyl complexes are the most stable of the three species, except for the norbornene, cyclopentene, and cyclohexene cases. In the latter two, the alkylidenes are slightly favored over the tuck-in alkyls.

While the rate of the niobium rearrangements correlates inversely with the expected stabilities of the olefin complexes, the tantalum results are less easy to interpret. Since the tuck-in alkyl intermediates are observed, consideration of a rate-determining step in going from olefin complex to alkylidene is no longer appropriate. In many cases, the first transition state has the highest free energy, yet $k_2 < k_1$ because of the stability of the tuck-in alkyl. In general, the tantalum rates are substantially faster than those of niobium, and the same rough trends exist, at least in the context of the olefin to alkylidene transformation. The styrenes and ethylene are the slowest, the propene and 1-butene are next, and the speedy rearrangements are the cyclics and norbornene.

Structure and Dynamics of (silox)$_3{}^n$BuTa(κ^2-O,C-OSi^{t}Bu$_2$-CMe$_2$CH$_2$) (6-^{n}Bu). X-ray diffraction quality crystals of the tantalum tuck-in butyl derivative, (silox)$_3{}^n$BuTa(κ^2-O,C-OSi^t-Bu$_2$CMe$_2$CH$_2$) (**6**-^{n}Bu), were obtained, and its molecular structure is given in Figure 3 along with pertinent bond distances and angles; further structural information is given in Supporting

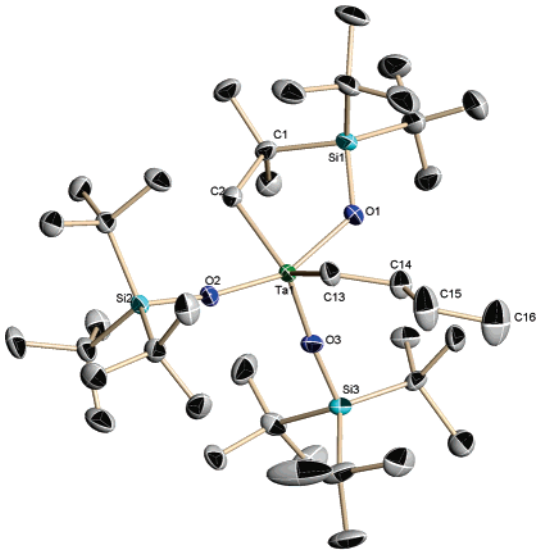

Figure 3. Molecular view of (silox)$_3$^{n}BuTa(κ^2-O,C-OSi^{t}Bu$_2$CMe$_2$CH$_2$) (**6**-^{n}Bu). Selected bond distances (Å) and angles (deg) not in text: C1−C2, 1.556(5); C13−C14, 1.520(5); C14−C15, 1.511(6); C15−C16, 1.521(7); Si1−O1, 1.676(3); Si2−O2, 1.674(2); Si3−O3, 1.682(2); O1−Ta−C13, 86.07(12); O2−Ta−C13, 88.48(12); Ta−C13−C14, 115.5(3); C13−C14−C15, 114.8(4); C14−C15−C16, 112.9(4); Ta−O2−Si2, 171.27(15); Ta−O3−Si3, 174.98(16).

Information. **6**-^{n}Bu is best described as a distorted trigonal bipyramid, with the less electronegative alkyl substituents, cyclometalated C2 and ^{n}Bu C13, and silox O3 occupying the equatorial plane (/O3−Ta−C2 = 121.06(13)°, /O3−Ta−C13 = 111.41(13)°, and /C2−Ta−C13 = 127.10(15)°).[52] The remaining silox groups are pseudoaxial, with /O1−Ta−O2 = 154.06(10°), and d(Ta−O1) = 1.937(2) Å and d(Ta−O2) = 1.920(2) Å, which are longer than the equatorial d(Ta−O3) of 1.878(2) Å, as expected. The bite angle of the cyclometalated unit (/O1−Ta−C2 = 78.84(12)°) is less than 90°, and the remaining angles of the five-membered ring manifest significant strain (/Ta−O1−Si1 = 128.34(14)°, /O1−Si1−C1 = 97.97-(14)°, /Si1−C1−C2 = 101.9(2)°, /Ta−C2−C1 = 118.8(2)°) in comparison to normal silox geometric parameters. Despite this strain, the d(Ta−C2) of 2.211(3) Å is only slightly longer than the comparative butyl distance, d(Ta−C13) = 2.178(4) Å. The remaining axial/equatorial angles support the distorted tbp geometry and are consistent with intersilox steric repulsions being the most influential about the core.

The spectral signatures of the tuck-in alkyl complexes, (silox)$_3$(R)M(κ^2-O,C-OSi^{t}Bu$_2$CMe$_2$CH$_2$) (M = Nb, R = CH$_2$-CH$_2$^{t}Bu, **4**-CH$_2$CH$_2$^{t}Bu; Ta, **6**-R), indicate mirror symmetry, while the solid-state structure of (silox)$_3$^{n}BuTa(κ^2-O,C-OSi^{t}Bu$_2$-CMe$_2$CH$_2$) (**6**-^{n}Bu) is asymmetric. Variable temperature ^{1}H NMR spectroscopy on (silox)$_3$^{n}PrTa(κ^2-O,C-OSi^{t}Bu$_2$CMe$_2$CH$_2$) (**6**-^{n}Pr), chosen for ease of analysis, revealed three coalescence phenomena associated with the α-CH$_2$ (k = 1500 s^{-1} at T_c = 218 K, $\Delta G^{\ddagger}$ = 10.4(5) kcal/mol) and β-CH$_2$ (k = 730 s^{-1} at T_c = 221 K, $\Delta G^{\ddagger}$ = 9.9(5) kcal/mol) methylenes of the ^{n}Pr group, and the methylene (k = 300 s^{-1} at T_c = 223 K, $\Delta G^{\ddagger}$ = 9.5(5) kcal/mol) of the cyclometalation arm. The activation free energies affiliated with these resonances are consistent with the relatively low barriers common to axial and equatorial exchange mechanisms in five-coordination.[59]

Olefin to Alkylidene Mechanism. 1. Mechanistic Paths. The previous discussion regarding the rates and thermodynamics of the olefin to tuck-in alkyl to alkylidene rearrangement was predicated on the tuck-in alkyl as a viable intermediate. This need not be the case. As Scheme 3 shows, in some scenarios the tuck-in alkyl would be a side process of no consequence to the reaction of interest. For example, the olefin complex could rearrange via a one-step 1,2-H migration. Likewise, a vinylic CH bond activation, followed by a 1,3-H migration leads to the same product if the α-positions of the olefin were labeled. Since these processes are not readily distinguished, either constitutes an **H-transfer** path.

A second possibility arises from loss of olefin and cyclometalation of (silox)$_3$M (M = Nb, **1**; Ta, **2**) to the original tuck-in species, the hydride (silox)$_2$HM(κ^2-O,C-OSi^{t}Bu$_2$CMe$_2$CH$_2$) (M = Nb, **7**;[38] Ta, **8**).[42] Reinsertion of the olefin to afford the

Scheme 3

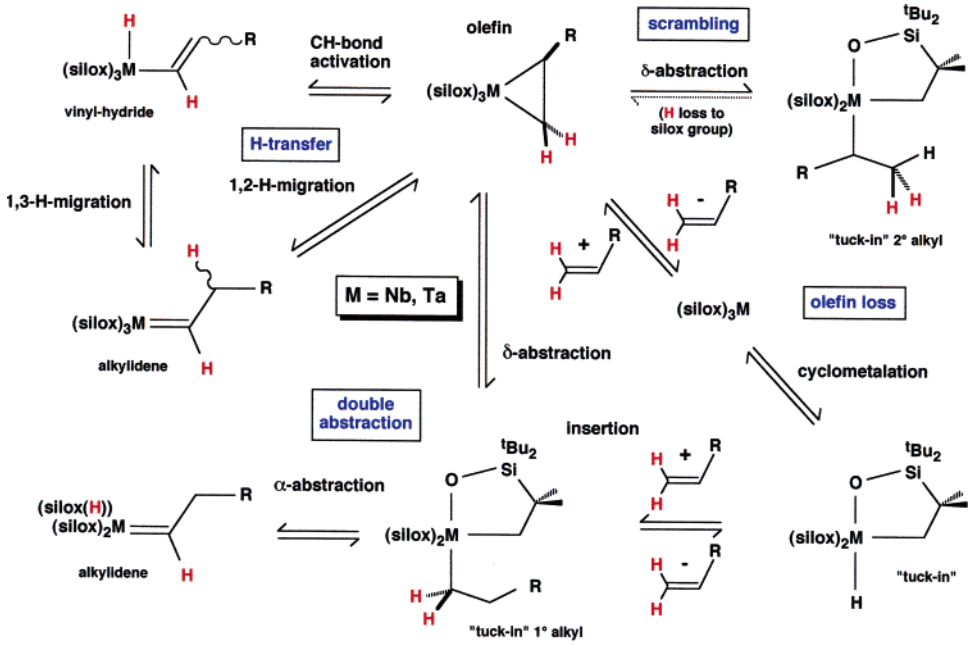

tuck-in alkyl, followed by an abstraction by the cyclometalation arm on the α-carbon of the primary alkyl, leads to the alkylidene. This path is termed the **olefin loss** mechanism.

The third possibility is the one implied previously. A *δ*-abstraction of a hydrogen from a silox CH bond by the *β*-carbon of the olefin can lead directly to the "tuck-in" alkyl. A subsequent α-abstraction by the cyclometalation arm on the primary alkyl provides the alkylidene. Consideration of this **double abstraction** path leads to another possibility. If a monosubstituted olefin were able to abstract hydrogen from a silox CH bond utilizing the unsubstituted α-carbon, a disubstituted alkylidene could result, *but none has been directly observed for monosubstituted olefin substrates.* More importantly, if *δ*-abstraction led to an intermediate tuck-in secondary alkyl, reversibility of this reaction—a *β*-abstraction by the cyclometalation arm on the alkyl—would eventually lead to loss of label from the α-positions of a monosubstituted olefin to the silox groups, which is referred to as **scrambling** in the scheme.

2. Elucidation. Previous experience with the cyclometalation of (silox)$_3$M (M = Nb, **1**; Ta, **2**) to (silox)$_2$HM(κ^2-O,C-OSi^{t}Bu$_2$CMe$_2$CH$_2$) (M = Nb, **7**;[38] Ta, **8**)[42] pointed toward the olefin loss path as a distinct possibility; hence various labeling experiments were devised to assess it. First, the perdeuterated ethylene complex, (silox)$_3$Nb(η-C$_2$D$_4$) (**1**-C$_2$D$_4$), was thermolyzed at 155 °C to probe for deuterium incorporation into the silox ligands (eq 9).

$$\underset{\mathbf{1}\text{-}C_2D_4}{(\text{silox})_3\text{Nb}(\eta\text{-}C_2D_4)} \underset{155\ ^\circ\text{C}}{\overset{\text{benzene-}d_6}{\rightleftharpoons}} (\text{silox})_2[{}^t\text{Bu}_2(\text{Me}_2\text{CCH}_{3-x}/\text{D}_x)\text{SiO}]\text{Nb}{=}\underset{\mathbf{1}{=}\text{CHMe-}d_4}{\text{C}(\text{H}/\text{D}_y)\text{CH}_{3-z}/\text{D}_z} \quad (9)$$

After 12 h, deuterium was indeed distributed in all three sites, and after 24 h, 96% of the deuterium was present in the silox ligands according to ^{2}H NMR spectroscopy.

Next, the ^{13}C-labeled ethylene complex, (silox)$_3$Nb(η-^{13}C$_2$H$_4$) (**1**-^{13}C$_2$H$_4$), was thermolyzed at 155 °C in the presence of ∼5 equiv of nonlabeled ethylene (eq 10).

$$\underset{\mathbf{1}\text{-}{}^{13}C_2H_4}{(\text{silox})_3\text{Nb}(\eta\text{-}{}^{13}C_2H_4)} + C_2H_4 \underset{155\ ^\circ\text{C}}{\overset{\text{benzene-}d_6}{\rightleftharpoons}} \underset{\mathbf{1}\text{-}C_2H_4}{(\text{silox})_3\text{Nb}(\eta\text{-}C_2H_4)} + {}^{13}C_2H_4 \quad (10)$$

Once the equilibrium $K_{alk/ole}$ of ∼0.35 was reached, only 30% of the ethylene and alkylidene complexes retained the label, indicating that olefin exchange occurred on a similar time scale as the rearrangement.[45] When the propene derivative (silox)$_3$Nb(η-C$_2$H$_3$Me) (**1**-C$_2$H$_3$Me) was heated in the presence of ∼10 equiv of ethylene (eq 11), about 50% of **1**-C$_2$H$_4$ formed within 27 min and within 64 min, 90% conversion to the ethylene complex was noted along with 8% (silox)$_3$Nb=CHEt (**1**=CHEt) and 2% (silox)$_3$Nb=CHMe (**1**=CHMe).

$$\underset{\mathbf{1}\text{-}C_2H_3Me}{(\text{silox})_3\text{Nb}(\eta\text{-}C_2H_3Me)} + C_2H_4 \underset{155\ ^\circ\text{C}}{\overset{\text{benzene-}d_6}{\rightleftharpoons}} \underset{\mathbf{1}\text{-}C_2H_4}{(\text{silox})_3\text{Nb}(\eta\text{-}C_2H_4)} + C_2H_3Me \quad (11)$$

The **1**-C$_2$H$_3$Me + C$_2$H$_4$ experiment is consistent with the olefin loss pathway, provided either the insertion or the α-abstraction steps are rate-determining, since ethylene would be expected to trap (silox)$_3$Nb (**1**), precursor to the tuck-in (silox)$_2$HNb(κ^2-O,C-OSi^{t}Bu$_2$CMe$_2$CH$_2$) (**7**), faster than propene would rebind. In contrast, if the same criteria were applied to the ^{13}C$_2$H$_4$ experiment, loss of labeled ethylene from the starting complex should be greater than observed; thus the olefin loss path was considered unlikely. No order in cyclohexene was observed when the rearrangement of (silox)$_3$Nb(η-^{c}C$_6$H$_{10}$) (**2**-^{c}C$_6$H$_{10}$) was conducted in the presence of excess (19 equiv) olefin.

Thermolysis (103 °C, ∼4 h) of cyclopentene adduct (silox)$_3$Ta(η-^{c}C$_5$H$_8$) (**2**-^{c}C$_5$H$_8$) with ∼15 equiv of ethylene present afforded only the two rearrangement products: tuck-in cyclopentyl (silox)$_2$(^{c}Pe)Ta(κ^2-O,C-OSi^{t}Bu$_2$CMe$_2$CH$_2$) (**6**-Pe, 36%) and cyclopentylidene (silox)$_3$Ta=^{c}C$_5$H$_8$ (**2**=^{c}C$_5$H$_8$, 48%, eq 12).

$$\underset{\mathbf{2}\text{-}{}^cC_5H_8}{(\text{silox})_3\text{Ta}(\eta\text{-}{}^cC_5H_8)} + C_2H_4 \rightleftharpoons \mathbf{6}\text{-}{}^c\text{Pe} + C_2H_4 \rightleftharpoons \underset{\mathbf{2}{=}{}^cC_5H_8}{(\text{silox})_3\text{Ta}{=}{}^cC_5H_8} + C_2H_4 \quad (12)$$

It was expected that the olefin loss path would permit ethylene incorporation via trapping of (silox)$_3$Ta (**2**) or (silox)$_2$HTa(κ^2-O,C-OSi^{t}Bu$_2$CMe$_2$CH$_2$) (**8**), but on the off-chance that the cyclopentene-derived species were thermodynamically more stable than those produced from ethylene, the complementary experiment was conducted. When the ethylene complex was heated at 103 °C with 56 equiv of ^{c}C$_5$H$_8$ present, the tuck-in ethyl, (silox)$_2$EtTa(κ^2-O,C-OSi^{t}Bu$_2$CMe$_2$CH$_2$) (**6**-Et), and alkylidene **2**=CHMe formed with no evidence of cyclopentene-derived products (eq 13).

$$\underset{\mathbf{2}\text{-}C_2H_4}{(\text{silox})_3\text{Ta}(\eta\text{-}C_2H_4)} + {}^cC_5H_8 \rightleftharpoons \mathbf{6}\text{-Et} + {}^cC_5H_8 \rightleftharpoons \underset{\mathbf{2}{=}\text{CHMe}}{(\text{silox})_3\text{Ta}{=}\text{CHMe}} + {}^cC_5H_8 \quad (13)$$

The lack of olefin exchange in the tantalum system rules out the possibility of olefin loss as a viable mechanistic path. By inference, and with careful observation of the qualitative rearrangement and exchange rates in eqs 10 and 11, the olefin loss mechanism is also eliminated for niobium.

The tuck-in hydride, (silox)$_2$HTa(κ^2-O,C-OSi^{t}Bu$_2$CMe$_2$CH$_2$) (**8**) was heated at 103 °C with 10 equiv of ethylene, and after 23 min 57% of the tuck-in ethyl **6**-Et was generated along with **2**-C$_2$H$_4$ (26%) and **2**=CHMe (3%). Since it is unlikely that **8** reverts to (silox)$_3$Ta (**2**) under these conditions,[38] it is assumed that the **2**-C$_2$H$_4$:**2**=CHMe product ratio is generated from **6**-Et. The 1.6(3) kcal/mol difference given by the 8.7:1 ratio at 103 °C is between the predicted $\Delta\Delta G^{\ddagger} \approx 2.7$ kcal/mol that corresponds to a kinetic product ratio of ∼37:1 and the $\Delta G°$ of 1.1 kcal/mol, which represents the thermodynamic 4.4:1 ratio.

(59) Casanova, D.; Cirera, J.; Llunell, M.; Alemany, P.; Avnir, D.; Alvarez, S. *J. Am. Chem. Soc.* **2004**, *126*, 1755−1763.

Scheme 4

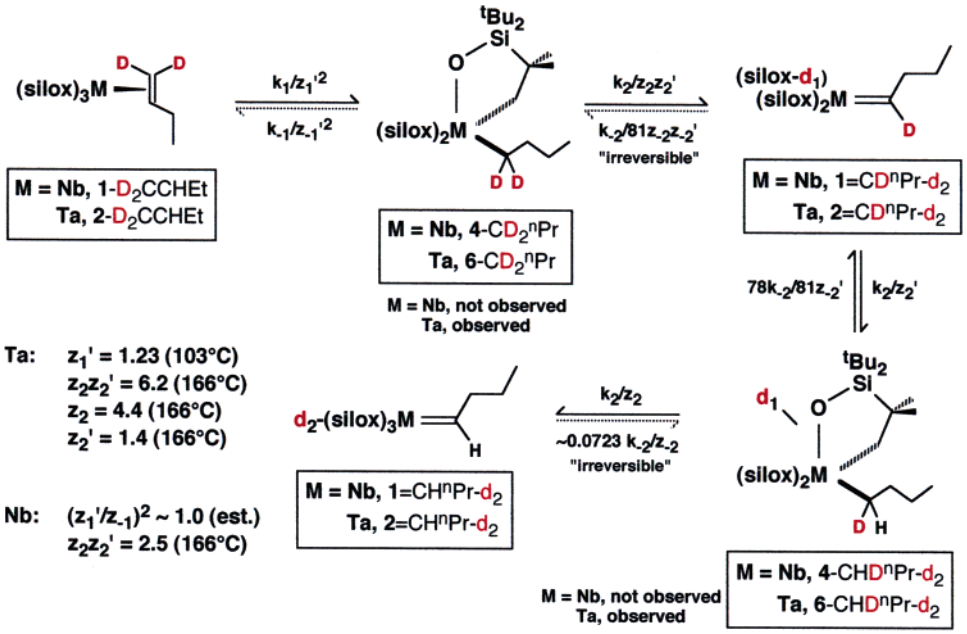

The direct H-transfer paths proposed in Scheme 3 can be differentiated from the double abstraction path by labeling the α-positions of the olefin adduct with deuterium. The H-transfer mechanisms lead to a α,β-dideuterio alkylidene product, whereas double abstraction affords an α-deuterated alkylidene that has a deuterium incorporated into a silox group. Note that this experiment can go awry if reversible δ-abstraction by the olefin α-carbon enables scrambling into the silox groups prior to rearrangement (Scheme 3, scrambling). Since the 1-butene conversion conveniently stops at the tuck-in butyl (**6**-^{n}Bu) at 103 °C, α,α-dideuterio-1-butene[60] was chosen as a convenient assay, as Scheme 4 illustrates. Rearrangement of (silox)$_3$Ta(η-D$_2$CCHEt) (**2**-D$_2$CCHEt) at 103 °C afforded the tuck-in α,α-dideuterio-butyl, (silox)$_2$(^{n}PrCD$_2$)Ta(κ^2-O,C-OSi^{t}Bu$_2$CMe$_2$CH$_2$) (**6**-CD$_2{}^n$Pr), with no detectable deuterium loss from the α-positions according to ^{1}H NMR spectroscopy. A significant normal secondary isotope effect of $z_1' = 1.23$ ($z_1' = k_H/k_D$,[61,62] observed $z_1'^2 = 1.52$; the two α-positions were assumed to have the same secondary effect) was determined for the δ-abstraction event by comparison of an all-protio sample run in conjunction with the dideuterio probe.

Monitoring the ensuing formation of (silox)$_2$(silox-d_1)-Ta=CD^{n}Pr (**2**=CD^{n}Pr-d_2) at 166 °C was more complicated, but beneficially so. While the α-abstraction can be treated as irreversible because the deuterium is lost to 81 equivalent positions of the three silox groups, the pseudo-reversible process of δ-abstraction by the alkylidene affords (silox)$_{2-x}$(silox-d_1)$_x$-(^{n}PrCHD)Ta(κ^2-O,C-OSi^{t}Bu$_2$CMe$_2$CH$_2$)$_{1-y}$(κ^2-O,C-OSi^{t}Bu$_2$-CMe$_2$CH$_2$-d_1)$_y$ ($x + y = 1$, **6**-CHD^{n}Pr-d_2), which contains one deuterium in the α-carbon of the ^{n}Bu and another among the *tert*-butyl groups of the silox ligands and the cylometalated silox. α-Abstraction of deuterium leads to (silox)$_{3-(2-x)}$(silox-d_1)$_{2-2x}$-(silox-d_2)$_x$Ta=CH^{n}Pr ($0 < x < 1$, **2**=CH^{n}Pr-d_2), which is also essentially irreversible (the ~0.0723 k_{-2}/z$_{-2}$ in Scheme 4 reflects a statistical estimate of the sum of reversible CDH$_2$ and CD$_2$H δ-abstractions by the alkylidene). By knowing k_2 and k_{-2} from monitoring, in tandem, the perprotio sample, the isotope effects may be broken down with simulation of all relevant processes. The first α-abstraction rate is influenced by a primary KIE (z_2) and an α-secondary KIE (z_2') such that $z_2z_2' = 6.2$, but the second α-abstraction KIE— loss of D from **6**-CHD^{n}Pr-d_2—is uncomplicated by secondary effects. By ^{1}H NMR spectroscopic monitoring of the growth of the alkylidene hydrogen of **2**=CH^{n}Pr-d_2, a z_2 of 4.4 was revealed, a value comparable to other abstractions,[63−76] especially when taking account of the high temperature. The α-secondary KIE is substantial ($z_2' = 1.4 = 6.5/4.4$) but certainly within reason.

The transparency of the KIEs in the tantalum system provides a benchmark for comparison with the niobium system in which the lack of an observable tuck-in alkyl intermediate renders identification of the rate-determining step problematic. The KIE

(60) Budzikiewicz, H.; Bold, P. *Org. Mass. Spectrom.* **1991**, *26*, 709−712.
(61) Carpenter, B. K. *Determination of Reaction Mechanisms*; Wiley-Interscience: New York, 1984.
(62) Melander, L.; Saunders, W. H., Jr. *Reaction Rates of Isotopic Molecules*; Wiley-Interscience: New York, 1980.
(63) Fryzuk, M.; Duval, P.; Mao, S.; Zaworotko, M.; MacGillivray, L. *J. Am. Chem. Soc.* **1999**, *121*, 2478−2487; $z = 3.0$ at 343 K.
(64) Wood, C. D.; McLain, S. J.; Schrock, R. R. *J. Am. Chem. Soc.* **1979**, *101*, 3210−3222; $z = 6.0$ at 309 K.
(65) Schrock, R. R.; Fellmann, J. D. *J. Am. Chem. Soc.* **1978**, *100*, 3359−3370; $z = 2.7$ at 348 K.
(66) Cheon, J.; Rogers, D.; Girolami, G. *J. Am. Chem. Soc.* **1997**, *119*, 6804−6813; $z = 5.2$ at 378 K.
(67) McDade, C.; Green, J. C.; Bercaw, J. E. *Organometallics* **1982**, *1*, 1629−1634; $z = 2.9$ at 371 K.
(68) Pamplin, C. B.; Legzdins, P. *Acc. Chem. Res.* **2003**, *36*, 223−233; $z = 2.4$, 364 K.
(69) Buchwald, S. L.; Nielsen, R. B. *J. Am. Chem. Soc.* **1988**, *110*, 3171−3175; $z = 5.2$ at 353 K.
(70) Schock, L. E.; Brock, C. P.; Marks, T. J. *Organometallics* **1987**, *6*, 232−241; $z = 6.5$ at 343 K.
(71) Luinstra, G. A.; Teuben, J. H. *Organometallics* **1992**, *11*, 1793−1801; $z = 5.1$ at 353 K, 5.7 at 315 K.
(72) Bruno, J. W.; Smith, G. M.; Marks, T. J.; Fair, C. K.; Schultz, A. J.; Williams, J. M. *J. Am. Chem. Soc.* **1986**, *108*, 40−56.
(73) Mayer, J. M.; Curtis, C. J.; Bercaw, J. E. *J. Am. Chem. Soc.* **1983**, *105*, 2651−2660; $z = 9.7$ at 298 K.
(74) Bulls, A. R.; Schaefer, W. P.; Serfas, M.; Bercaw, J. E. *Organometallics* **1987**, *6*, 1219−1226; $z = 2.5$ at 413 K.
(75) Bennett, J. L.; Wolczanski, P. T. *J. Am. Chem. Soc.* **1997**, *119*, 10696−10719; $z = 7.4$, 13.7 at 298 K, 5.6 at 363 K.
(76) Schaller, C. P.; Cummins, C. C.; Wolczanski, P. T. *J. Am. Chem. Soc.* **1996**, *118*, 591−611; $z = 6.3$, 7.1, 4.6 at 370 K.

Scheme 5

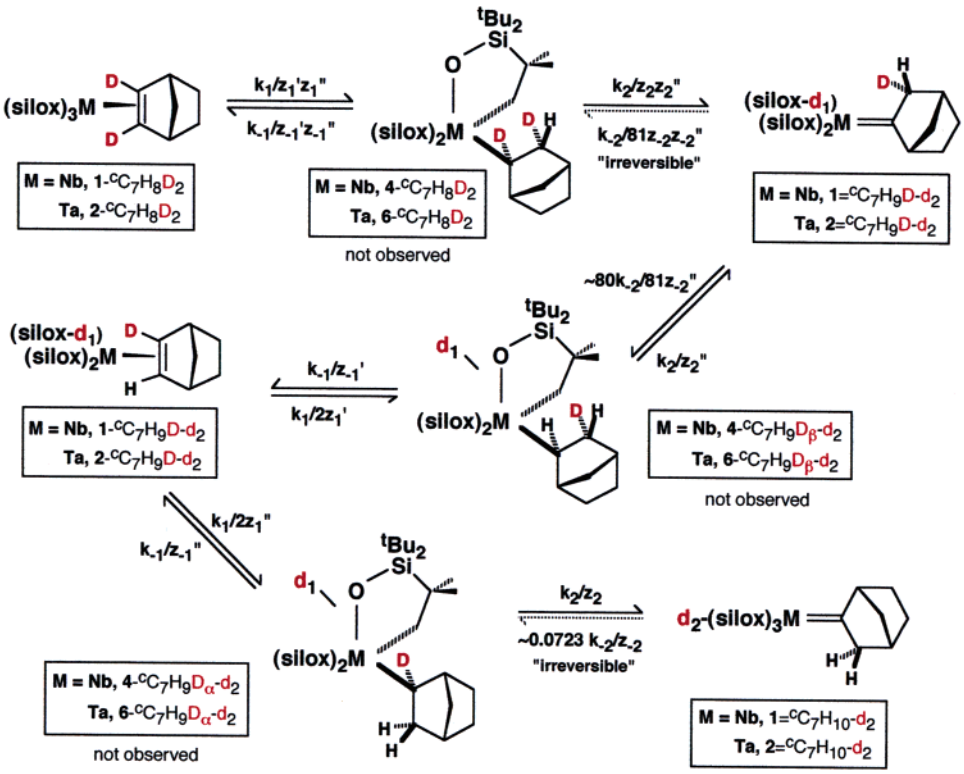

for k_f, which corresponds to the conversion of (silox)$_3$Nb(η-D$_2$CCHEt) (**1**-D$_2$CCHEt) to (silox)$_2$(silox-d_1)Nb=CD^{n}Pr (**1**=CD^{n}Pr-d_2), was observed to be 2.5 at 166 °C. If formation of the presumed tuck-in butyl (silox)$_2$(^{n}PrCD$_2$)Nb(κ^2-O,C-OSi^{t}Bu$_2$CMe$_2$CH$_2$) (**4**-CD$_2{}^n$Pr) were rate-determining, the KIE should be ≤1.5, which was the value in the tantalum system (i.e., $z_1'^2 = (1.23)^2$) at 103 °C. For the value of 2.5 to be attributable to formation of the tuck-in butyl, a secondary isotope effect of about 1.6 would need to be invoked, and this is outside the normal range,[61,62] especially when taking account of the high temperature. The value establishes α-abstraction as the rate-determining step in the Nb double abstraction mechanism. Since secondary *equilibrium* isotope effects (z_1'/z_{-1}') are expected to be ~1.0, the z_f of 2.5 for Nb is approximately z_2z_2', which in the tantalum case was 6.2. Conventionally, the lower value for Nb would be ascribed to a less-symmetric transition state for H/D transfer. Since the tuck-in butyl is not observed for Nb, the transition state for conversion to the alkylidene should come earlier than in the tantalum case where the intermediate and butylidene are within $\Delta G° < 1.0$ kcal/mol at 166 °C.

The phenyl ring renders the styrene systems different from the other monosubstituted olefins; thus an attempt to measure isotope effects was made similar to Scheme 4. A thermolysis of (silox)$_3$Ta(η-D$_2$CCHPh) (**2**-D$_2$CCHPh)[77] was conducted in tandem with **2**-C$_2$H$_3$Ph. Simulation of the concentration vs time profiles of the various labeled intermediates failed to yield tenable rate constants and isotope effects. In reviewing the data, the more rapid than expected growths of (silox)$_{2-x}$(silox-d_1)$_x$(PhCH$_2$CHD)Ta(κ^2-O,C-OSi^{t}Bu$_2$CMe$_2$CH$_2$)$_{1-y}$(κ^2-O,C-OSi^{t}Bu$_2$CMe$_2$CH$_2$-d_1)$_y$ ($x + y = 1$, **6**-CHDCH$_2$Ph-d_2) and (silox)$_2$(silox-d_1)Ta(η-DHCCHPh) (**2**-DHCCHPh-d_2) were responsible for the difficulty in data fitting. Note that reversible cyclometalation to the tuck-in secondary alkyl, (silox)$_{2-x}$(silox-d_1)$_x$(PhCH$_2$CHD)((CD$_2$H)PhHC)Ta(κ^2-O,C-OSi^{t}Bu$_2$CMe$_2$CH$_2$)$_{1-y}$(κ^2-O,C-OSi^{t}Bu$_2$CMe$_2$CH$_2$-d_1)$_y$ ($x + y = 1$, **6**-CHPh(CD$_2$H)), can cause loss of label to the silox groups *prior to formation of the alkylidene*, as indicated by the scrambling path in Scheme 3. Unfortunately, since there were no practical independent means of monitoring the scrambling process, inclusion of these steps into the simulations do not solve the analytical problems. Nevertheless, the inability to fit the styrene labeling experiments is strong evidence for the presence of the scrambling path in this instance. The tuck-in secondary alkyl **6**-CHPh(CD$_2$H) is unique because of the α-phenyl substituent that will inductively stabilize the tantalum alkyl bond, which is polarized Ta$^{\delta+}$-C$^{\delta-}$HPh(CD$_2$H). Similar reasoning has been used to explain the unusual stability of metal-benzyl bonds in early metal C−H activation systems.[75,76]

The absence of a tuck-in alkyl intermediate in the case of norbornene might be ascribed to a different mechanism. However, at 103 °C, rearrangement of (silox)$_3$Ta(η-^{c}C$_7$H$_8$D$_2$) (**2**-^{c}C$_7$H$_8$D$_2$), which was labeled with deuterium in the olefinic positions,[78−80] afforded the β-deuterio norbornylidene, (silox)$_2$(silox-d_1)Ta=^{c}C$_7$H$_9$D (**2**=^{c}C$_7$H$_9$D-d_2), consistent with the established pathway. Had a hydride transfer path been operable, the β,β-dideuterio norbornylidene would have been produced, but ^{1}H and ^{2}H NMR spectroscopy established the β-CH$_{exo}$D$_{endo}$ group and revealed a deuterium in a silox ligand. The rearrangement of **2**-^{c}C$_7$H$_8$D$_2$ is complicated but informative, as Scheme 5 shows. The isotope effect for k_f was 2.96(3), which indicated that the α-abstraction step is rate-determining. If formation of the tuck-in alkyl is construed as two sp^2 → sp^3

(77) Fischetti, W.; Heck, R. F. *J. Organomet. Chem.* **1985**, *293*, 391−405.
(78) Stille, J. K.; Sonnenberg, F. M. *J. Am. Chem. Soc.* **1966**, *88*, 4915−4921.
(79) Chamberlin, A. R.; Stemke, J. E.; Bond, F. T. *J. Org. Chem.* **1978**, *43*, 147−155.
(80) Bond, F. T.; DiPietro, R. A. *J. Org. Chem.* **1981**, *46*, 1315−1318.

changes (π-back-bonding presumably renders the norbornene olefin carbons between sp^2- and sp^3-hybridization), each contributes a small inverse isotope effect for the k_1 step (δ-abstraction), but the reverse (k_{-1}) process should contain two normal secondary isotope effects.[61,62] The EIE for tuck-in alkyl formation should be inverse. Consequently, the KIE for α-abstraction, which contains primary and β-secondary isotope effects (i.e., z_2z_2''), should actually be >2.96(3), and this value is clearly in line with that obtained for 1-butene.

Note that the remainder of the scheme for label loss reveals a stereochemical question. One can assume the loss of label from the alkylidene of **2**=^{c}C$_7$H$_9$D-d_2 occurs via a microscopically reversible path: (1) a CH bond (neglecting α-secondary effects on 2/81 silox methyl hydrogens, the rate is $\sim 80k_{-2}/81z_{-2}''$) of a silox adds to the endo-face of the alkylidene (another δ-abstraction, but by the alkylidene) to give (silox)$_{2-x}$(silox-d_1)$_x$(^{c}C$_7$H$_9$D$_\beta$)Ta(κ^2-O,C-OSi^{t}Bu$_2$CMe$_2$CH$_2$)$_{1-y}$(κ^2-O,C-OSi^{t}Bu$_2$CMe$_2$CH$_2$-d_1)$_y$ ($x + y = 1$, **6**-^{c}C$_7$H$_9$D$_\beta$-d_2); (2) β-abstraction occurs only from the exo-face to give (silox)$_2$(silox-d_1)Ta(η-^{c}C$_7$H$_9$D) (**2**-^{c}C$_7$H$_9$D-d_2) with k_{-1}/z_{-1}' as the rate; (3) a δ-abstraction generates the tuck-in alkyl across the exo-face with a rate reflecting the 50% probability of correct olefin orientation ($k_1/2z_1$); and (4) an essentially irreversible α-abstraction (k_2/z_2) to afford **2**=^{c}C$_7$H$_{10}$-d_2. A fit of the data assuming this path affords an overall KIE of 1.08(1) consistent with a rate-determining k_{-2} step as expected. Addition of nucleophiles to 2-norbornanone occurs toward both faces, with a slight preference toward the exo-side;[81] hence addition to the exo-face is possible. However, such a path ultimately leads to an endo-olefin species, which is expected to be heavily disfavored relative to the exo-isomer.[82]

As in the butene rearrangements, the tantalum norbornene case is helpful in assessing the corresponding niobium chemistry. Thermolysis of (silox)$_3$Nb(η-^{c}C$_7$H$_8$D$_2$) (**1**-^{c}C$_7$H$_8$D$_2$) provided the β-deuterio norbornylidene, (silox)$_2$(silox-d_1)Nb=^{c}C$_7$H$_9$D (**2**=^{c}C$_7$H$_9$D-d_2), consistent with the double abstraction pathway. At 166 °C, the k_H/k_D of the rearrangement was 2.3(2), a value commensurate with the butene case, and one best accommodated by a rate-determining α-abstraction, as explained for the tantalum rearrangement. If this is true, scrambling of the β-deuterium of the norbornylidene in **2**=^{c}C$_7$H$_9$D-d_2 to a silox group should occur with k_{-2} (δ-abstraction by the norbornylidene) as the rate-determining step. By fitting the **1**-^{c}C$_7$H$_8$D$_2$ to **2**=^{c}C$_7$H$_9$D-d_2 to d_2-(silox)$_3$Nb=^{c}C$_7$H$_{10}$ (**1**=^{c}C$_7$H$_{10}$-d_2) rearrangements and assuming the standard mechanism shown in Scheme 5, the loss of the β-D occurred with a k_r of 6.17(7) $\times 10^{-6}$ s^{-1} at 166 °C ($\Delta G_r^{\ddagger} = 36.5(1)$ kcal/mol). The rearrangement occurs with a standard free energy change of $-4.5(1)$ kcal/mol at 166 °C, which is approximately -3.9 kcal/mol at 103 °C, given the usual assumptions.

If the α-abstraction is the rate-determining step in the rearrangement of (silox)$_3$Nb(η-^{c}C$_6$H$_8$-1,2-D$_2$) (**1**-^{c}C$_6$H$_8$-1,2-D$_2$), the deuterium labels in the olefinic positions[83] should scramble within the cyclohexene prior to or at least competitively with formation of the alkylidene, (silox)$_2$(silox-d)Nb=^{c}C$_6$H$_9$-2-D-d_2 (**1**=^{c}C$_6$H$_9$-2-D-d_2), as Scheme 6 illustrates. At early conversion, where ~1% of the alkylidene has formed, the ratio of the

Scheme 6

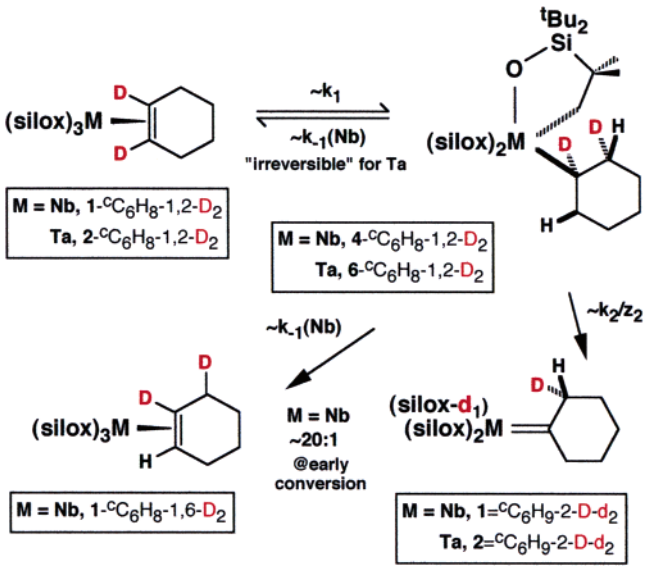

scrambled 1,6-D$_2$-cyclohexene complex, (silox)$_3$Nb(η-^{c}C$_6$H$_8$-1,6-D$_2$) (**1**-^{c}C$_6$H$_8$-1,6-D$_2$), which was formed upon β-H elimination, to the alkylidene is roughly 20:1. That product ratio is approximately the kinetic ratio $k_{-1}/k_2/z_2$, and if the primary isotope for abstraction is the same as that in the norbornene case ($z_2 \approx 2.4$ at 103 °C), then the product ratio is ~8.3 and $\Delta\Delta G^{\ddagger} = \Delta G_2^{\ddagger} - \Delta G_{-1}^{\ddagger} \approx 1.6$ kcal/mol. Unfortunately, analytical difficulties prevented the extraction of isotope effects in the Nb case, but the qualitative message is clear.

In the case of tantalum, Table 2 indicates that the rearrangement of (silox)$_3$Ta(η-^{c}C$_6$H$_8$-1,2-D$_2$) (**2**-^{c}C$_6$H$_8$-1,2-D$_2$) to (silox)$_2$-(1,2-D$_2$-^{c}C$_6$H$_8$)Ta(κ^2-O,C-OSi^{t}Bu$_2$CMe$_2$CH$_2$) (**6**-^{c}C$_6$H$_8$-1,2-D$_2$) is essentially irreversible; thus no deuterium is expected to scramble in the cyclohexene complex since rearrangement of **6**-^{c}C$_6$H$_8$-1,2-D$_2$ to (silox)$_2$(silox-d)Ta=^{c}C$_6$H$_9$-2-D-d_2 (**2**-^{c}C$_6$H$_9$-2-D-d_2) occurs more quickly. While **6**-^{c}C$_6$H$_8$-1,2-D$_2$ could not be assayed with confidence, ^{2}H NMR spectroscopy confirmed that the deuterium labels were in the silox ligand and the β-position of the **2**-^{c}C$_6$H$_9$-2-D-d_2, and no deuterium scrambling in the cyclohexene complex was detected.

Equilibria in the Niobium System. 1. Olefin Exchange. In contrast to tantalum, niobium olefin complexes (silox)$_3$Nb(ole) (**1**-ole) typically undergo substitution with free olefins faster than their rearrangements, or at least on the same time scale.[45] By measuring various equilibria, the relative stabilities of the olefin and alkylidene complexes were established and compared with those calculated for the models (HO)$_3$Nb(ole) (**1**′-ole). Where possible, **1**-ole complexes were subjected to concentrations of free olefin that enabled measurement of $K_{ole'/ole}$ = [**1**-ole′][ole]/[**1**-ole][ole′] by direct integration of all four species (eq 14).

$$\underset{\textbf{1}\text{-ole}}{(\text{silox})_3\text{Nb(ole)}} + \text{ole}' \overset{103\ ^\circ\text{C}}{\rightleftharpoons} \underset{\textbf{1}\text{-ole}'}{(\text{silox})_3\text{Nb(ole}')} + \text{ole} \qquad (14)$$

With little competing formation of the respective alkylidene compounds, a number of equilibria could be measured in this fashion, as Table 3 shows. Only the relative energy of (silox)$_3$Nb(η-^{c}C$_6$H$_{10}$) (**1**-^{c}C$_6$H$_{10}$) could not be determined, but given the accuracy of the *relative* energies of the computational

(81) Ohwada, T. *Tetrahedron* **1993**, *49*, 7649−7656.
(82) (a) Clavell, K. J. *Coord. Chem. Rev.* **1996**, *155*, 209−243. (b) Yamamoto, Y.; Ohno, T.; Itoh, K. *Organometallics* **2003**, *22*, 2267−2272.
(83) Ahlgren, G.; Akermark, B. *Acta Chem. Scand.* **1968**, *22*, 1129−1132.

Table 3. Equilibrium Measurements (K, $\Delta G°$ (kcal/mol) for (silox)$_3$Nb(ole) (**1**-ole) + ole′ ⇌ (silox)$_3$Nb(ole′) (**1**-ole′) + ole (103 °C, $\Delta G°$(ole′/ole), eq 14) and (silox)$_3$Nb(ole) (**1**-ole) + ole′ ⇌ (silox)$_3$Nb(alk′) (**1**═alk′) + ole (155 °C, $\Delta G°$(alk′/ole), eq 15, Corrected to 103 °C); Calculated Equilibria at 103 °C

reaction	K	$\Delta G°$ (ole′/ole)	$\Delta G_{calcd}°$ (ole′/ole)[a]	$\Delta G_{155}°$ (alk′/ole)	$\Delta G_{103}°$ (alk′/ole)	$\Delta G_{calcd}°$ (alk′/ole)[b]
1-C_2H_3Et + C_2H_3Me ⇌ **1**-C_2H_3Me + C_2H_3Et	0.76(1)	0.2	0.0			
1-C_2H_3Et + C_2H_3Ph ⇌ **1**-C_2H_3Ph + C_2H_3Et	17.3(5)	−2.1	−2.0			
1-C_2H_3Et + $^cC_7H_{10}$ ⇌ **1**-$^cC_7H_{10}$ + C_2H_3Et	2.18(5)	−0.58	−0.1			
1-$^cC_5H_8$ + C_2H_3Et ⇌ **1**-C_2H_3Et + $^cC_5H_8$	24.0(2)	−2.37	−3.0			
1-C_2H_4 + C_2H_3Ph ⇌ **1**-C_2H_3Ph + C_2H_4	0.0367(30)	2.5	2.5			
1-$C_2H_3{}^tBu$ + C_2H_3Et ⇌ **1**-C_2H_3Et + $C_2H_3{}^tBu$	9.73(8)	−1.7	*c*			
1-C_2H_3Ph + C_2H_3Ph-*p*-OMe ⇌ **1**-C_2H_3Ph-*p*-OMe + C_2H_3Ph	0.476(2)	0.55	*d*			
1-C_2H_3Ph + C_2H_3Ph-*p*-CF_3 ⇌ **1**-C_2H_3Ph-*p*-CF_3 + C_2H_3Ph	5.11(4)	−1.22	*e*			
1-C_2H_4 + C_2H_3Me ⇌ **1**═CHEt + C_2H_4	0.209(4)			1.33	1.85	8.9
1-C_2H_4 + C_2H_3Et ⇌ **1**═CH^nPr + C_2H_4	0.390(3)			0.80	1.32	8.8
1-C_2H_4 + $^cC_5H_8$ ⇌ **1**═$^cC_5H_8$ + C_2H_4	0.157(6)			1.57	2.09	9.7
1-C_2H_4 + $^cC_6H_{10}$ ⇌ **1**═$^cC_6H_{10}$ + C_2H_4	0.005(1)			4.5	5.0	9.6
1-C_2H_4 + $C_2H_3{}^tBu$ ⇌ **1**═$CHCH_2{}^tBu$ + C_2H_4	0.162(9)			1.55	2.07	c

[a] Calculations have an average deviation of −0.1(4) kcal/mol. [b] Calculations have an average deviation of +6.7(14) kcal/mol from the observed. [c] Calculations were not performed on (HO)$_3$Nb($C_2H_3{}^tBu$) (**1′**-$C_2H_3{}^tBu$ or **1′**═$CHCH_2{}^tBu$). [d] Calculations were not performed on (HO)$_3$Nb(C_2H_3Ph-*p*-OMe) (**1′**-C_2H_3Ph-*p*-OMe). [e] Calculations were not performed on (HO)$_3$Nb(C_2H_3Ph-*p*-CF_3) (**1′**-C_2H_3Ph-*p*-CF_3).

Table 4. Relative Observed, Estimated, and Calculated ((HO)$_3$Nb(olef) (1′-ole); (HO)$_3$Nb(alk) (**1′**═alk)) Standard Free Energies in kcal/mol (±0.2) at 103 °C for (silox)$_3$Nb(ole) (**1**-ole), (silox)$_3$Nb = (alk) (**1**═alk), and the (silox)$_3$Nb(ole) (**1**-ole) ⇌ (silox)$_3$Nb(alk) (**1**═alk) Rearrangement (Scheme 1); Activation Free Energies for $\Delta G^‡(k_f)$ and $\Delta G^‡(k_r)$ Are Included for Determination of Figure 4

reaction	$\Delta G°$ (ole)[a]	$\Delta G°$ (alk)[b]	$\Delta G^‡$ (k_f)	$\Delta G^‡$ (k_r)	$\Delta G°$ (alk/ole)	$\Delta G_{calcd}°$ (ole)[c]	$\Delta G_{calcd}°$ (alk/ole)
1-C_2H_4 ⇌ **1**═CHMe	0.0	1.6	35.5	33.9	1.6	0.0	2.6
1-C_2H_3Ph ⇌ **1**═$CHCH_2Ph$	2.5	3.2	35.5	34.8	0.7	2.5	8.5
1-$^cC_7H_{10}$ ⇌ **1**═$^cC_7H_{10}$	4.0	0.1	31.0	34.9	−3.9	4.4	−0.3
1-C_2H_3Et ⇌ **1**═CH^nPr	4.6	1.3	32.7	36.0	−3.3	4.5	4.3
1-C_2H_3Me ⇌ **1**═CHEt	4.8	1.9	33.4	36.3	−2.9	4.5	4.3
1-$C_2H_3{}^tBu$ ⇌ **1**═$CHCH_2{}^tBu$[d]	6.3	2.1	32.7	36.9	−4.2	e	e
1-$^cC_5H_8$ ⇌ **1**═$^cC_5H_8$	7.2	2.1	31.5	36.6	−5.1	7.5	2.1
1-$^cC_6H_{10}$ ⇌ **1**═$^cC_6H_{10}$	>8.4[f]	5.0	29.5	>32.9[f]	>−3.4[f]	10.9	−1.4

[a] Standard free energy of **1**-ole relative to that of **1**-C_2H_4 at 0.0 kcal/mol. [b] Standard free energy of **1**═alk relative to that of **1**-C_2H_4 at 0.0 kcal/mol. [c] Calculated standard free energy of **1′**-ole relative to that of **1′**-C_2H_4 at 0.0 kcal/mol; the average deviation is 0.1(3) kcal/mol. [d] Estimates of the standard free energy of (silox)$_2$($^tBuCH_2CH_2$)Nb(κ^2-O,C-$OSi^tBu_2CMe_2CH_2$) (**4**-$CH_2CH_2{}^tBu$) place it ∼2.1 kcal/mol. [e] Calculations were not performed on (HO)$_3$Nb($C_2H_3{}^tBu$) (**1′**-$C_2H_3{}^tBu$ or **1′**═$CHCH_2{}^tBu$). [f] Assuming the minimum amount of a substance that can be observed with confidence by ^{1}H NMR spectroscopy is 3%.

models pertaining to the remaining olefin complexes, its energy can be estimated with confidence.

2. Alkylidenes Relative to Olefin Complexes. Aside from the niobium ethylene and styrene rearrangments, the standard free energy changes could not be determined because the alkylidene proved to be too exoergic for the equilibria to be measured by NMR spectroscopic integration. In these instances, the relative energies of the alkylidenes could be obtained by measuring equilibria between lower energy olefin complexes and the **1**-alk of interest via eq 15.

$$\underset{\textbf{1}\text{-ole}}{(\text{silox})_3\text{Nb(ole)}} + \text{ole}' \overset{155\ °C}{\rightleftharpoons} \underset{\textbf{1}\text{-alk}}{(\text{silox})_3\text{Nb(alk}')} + \text{ole} \qquad (15)$$

At 155 °C, where the rearrangement is swifter, a judicious selection of free olefin permitted measurement of $K_{alk'/ole}$ = [**1**-alk′][ole]/[**1**-ole][ole′] by direct integration of all components, as Table 3 reveals. To correct to 103 °C, the standard entropy changes must be known. Epoxide to aldehyde/ketone isomerizations were considered as structural models that typically possess $\Delta S°$ values that range from +4 to +10 eu,[84] and the measured $\Delta S°$ for the niobium ethylene case was +12.5 eu. The latter measurement was given more weight; thus a compromise value of +10 was used to estimate cases needing entropy corrections.

The relative standard free energy of the norbornylidene, (silox)$_3$Nb═$^cC_7H_{10}$ (**1**═$^cC_7H_{10}$), could not be determined via equilibrium measurements because of interference from polymerization of the norbornene. However, in this circumstance, the KIE experiments above enabled the activation free energy for k_r to be determined (vide supra), and upon correcting to 103 °C, $\Delta G° = \Delta G_f^‡ - \Delta G_r^‡ = -3.9$ kcal/mol.

The data in Table 3 provide experimental relative standard free energies of (silox)$_3$Nb(ole) (**1**-ole) and (silox)$_3$Nb(alk) (**1**-alk) listed in Table 4, with the exceptions noted above. The smallest olefin, ethylene, and styrene, which possesses the electron-withdrawing Ph substituent, are the most tightly bound. Next is norbornene, presumably due to the diminution of ring strain[84,85] as back-bonding renders it more sp^3-like. 1-Butene and propene follow and bind with similar energies, while the hindered *tert*-butylethylene is more weakly attached. The hindered cyclic cases are the most weakly bound, with the smaller cyclopentene bound more tightly than cyclohexene by at least 1.2 kcal/mol, and more likely by around 3.7 kcal/mol, since the calculated number in this case is probably accurate. This is a typical list for the electron-rich Nb(III), with sterics favoring the smaller olefins, and olefins with electron-withdraw-

(84) For many rudimentary thermodynamics estimates, consult: http://webbook.nist.gov/chemistry/. For example, using Benson additivities (ref 85) and appropriate data, we found that the strain energies (E_s (±1−2 kcal/mol)) of pertinent molecules are: ^cPeH, 6.5; $^cC_5H_8$, 6.0; methylenecyclopentane, 5.3; ^cHexH, 0.3; $^cC_6H_{10}$, 1.6; cyclohexanone, 1.0; norbornane, 15.6; norbornene, 23(7); and 2-norbornanone, 14.3.

(85) Benson, S. W. *Thermochemical Kinetics*; Wiley & Sons: New York, 1968.

ing substituents being favored over those with greater electron donating capacity.

3. Calculations. Table 3 indicates that the equilibria of eq 14 were calculated fairly well, with an average deviation of −0.1(4) kcal/mol, but the experimental vs calculational olefins to alkylidene equilibria of eq 14 are poorly matched. If the calculated $\Delta G°$((HO)$_3$Nb(ole), **1′**-ole) values are referenced to **1**-C_2H_4 at 0.0 kcal/mol (Table 4), they match the experimental relative olefin energies quite well and possess an average deviation of 0.1(3) kcal/mol. This is expected, since it is basically complementary to the equilibria of eq 13. Likewise, the olefin/alkylidene equilibria for each substrate are poorly calculated, although a correction factor of −6.2(2.9) (−7.5(3) with the ethylene case left out) to each $\Delta G_{calcd}°$(alk/ole) would provide a decent fit to the experimental data. One possible explanation is that the olefin binding free energies, although relatively precise, may be overestimated: the calculated $\Delta G°$-(**1′**-ole) values (kcal/mol, relative to (HO)$_3$Nb (**1′**) + ole) are **1′**-C_2H_4, −27.7; **1′**-C_2H_3Ph, −25.2; **1′**-$^cC_7H_{10}$ (**1′**-nor), −23.3; **1′**-C_3H_6, **1′**-C_4H_8, −23.2; **1′**-$^cC_5H_8$, −20.2; **1′**-$^cC_6H_{10}$, −16.8. Preliminary olefin substitution kinetics suggests that the free energy of ethylene binding in **1**-C_2H_4 must be > −24 kcal/mol,[45] which suggests that the calculated ethylene binding energy in **1′**-C_2H_4 is too favorable. However, in the three measured cases (**1**-C_2H_4 → **1**=CHMe, $\Delta H°$ = 6.3; **2**-C_2H_4 → **2**=CHMe, $\Delta H°$ = 7.8; **2**-C_2H_3Ph → **2**=$CHCH_2$Ph, $\Delta H°$ = 10.4 kcal/mol), the calculated standard enthalpy change *underestimated* these values by −0.6, −3.4, and −2.6 kcal/mol. This is surprising, because steric factors are likely to attenuate the binding of olefins to a greater extent than the alkylidenes, and these influences are obviously not accounted for in the calculational model.[86]

While the olefin to alkylidene entropy change would be expected to favor the alkylidene, and this is corroborated in the measured cases (**1**-C_2H_4 → **1**=CHMe, $\Delta S°$ = 12.5(10) eu; **2**-C_2H_4 → **2**=CHMe, $\Delta S°$ = 16.6(16) eu; **2**-C_2H_3Ph → **2**=$CHCH_2$Ph, $\Delta S°$ = 25(1) eu), additional degrees of freedom in the alkylidene fragment vs the olefin do not contribute enough to account for the standard entropy change observed. The calculated entropy changes for the same cases are + 8.2, +5.3, and +2.1 eu, respectively. From these discrepancies, it is likely that entropic contributions from the silox groups upon rearranging from olefin to alkylidene are a principal reason the calculations are in error.

Discussion

Olefin to Alkylidene Rearrangement. 1. Mechanism. The mechanistic possibilities outlined in Scheme 3 have been pared by experiment, leaving the double abstraction pathway as the means by which (silox)$_3$M(ole) (M = Nb, **1**-ole; Ta, **2**-ole) rearranges to (silox)$_3$M(alk) (M = Nb, **1**=alk; Ta, **2**=alk). In coming to this conclusion, the niobium system is assumed to behave in a manner similar to tantalum, but with energetic differences. The most evident difference is the stability of the tuck-in alkyl intermediate, (silox)$_2$RM(κ^2-O,C-OSi^{t}Bu$_2$CMe$_2$-CH_2) (M = Nb, **4**−R; Ta, **6**-R), which is observed only for ole = *tert*-butylethylene in the niobium system, but is present in all but the norbornene rearrangement for tantalum.

The olefin loss pathway was eliminated by showing that excess olefin did not exchange into the tantalum system during the time scale of rearrangement, and a series of labeling experiments ruled out the simplest path, that of H-transfer. A competing reaction in which δ-abstraction leads to a tuck-in secondary alkyl can also be eliminated on the basis of labeling experiments for most substrates. However, the inability to fit rate data for the rearrangement of (silox)$_3$Ta(η-D_2CCHPh) (**2**-D_2CCHPh) is best accommodated in view of a competing scrambling path involving a tuck-in secondary alkyl intermediate. Rearrangements of the cyclic olefins—cyclopentane, cyclohexane, and norbornene—require the intermediacy of a tuck-in secondary alkyl species. It is surprising that secondary alkylidenes derived from acyclic substrates were not identified, especially since the energies of the cyclic alkylidenes suggest that such species should be close to (silox)$_3$M=CHR. It is doubtful that the transition state leading from a putative tuck-in secondary alkyl to secondary alkylidene would be problematic because rearrangements of the cyclics are relatively swift. It is more likely that the secondary akylidenes are unstable with respect to their primary counterparts. In the tantalum system, the tuck-in primary alkyls are the energetically dominant species; thus any tuck-in secondary alkyl may simply be relatively too high in energy to be easily discerned. For niobium, evidence for a tuck-in secondary alkyl was indirect; the 2-butene complex isomerized to the 1-butene species prior to the latter's rearrangment to butenylidene. Extended thermolyses (170 °C, >10 d) of (silox)$_3$Nb(ole) (ole = propene, **1**-C_2H_3Me; 1-butene, **1**-C_2H_3Et; styrene, **1**-C_2H_3Ph) failed to elicit any evidence of secondary alkylidenes. Since their formation is kinetically viable, it can be concluded that such species are roughly 4 kcal/mol above primary alkylidenes in energy.

Calculations performed on :CHEt and :CMe_2[87] provide a plausible reason for the relative instability of the secondary alkylidenes. The singlet ground state of :CMe_2 is ∼8.6 kcal/mol below that of the primary carbene, whose ground state is actually a triplet by ∼1.1 kcal/mol. Hyperconjugation of the six CH bonds into the empty p-orbital of the singlet state renders it substantially lower in energy than :CHEt. These same interactions may tend to destabilize any secondary metal-alkylidene because the p-orbital is now involved in π-bonding and 4e$^-$ interactions from the CH bonds will now be repulsive in character. Entropic factors pertaining to the silox groups may also disfavor secondary alkylidenes.

Scheme 7 illustrates the transition state for δ-abstraction[68,72,88−90] leading to the tuck-in alkyl intermediate and the subsequent α-abstraction[22,23,63−69] transition state that leads to the alkylidene product. The δ-abstraction (k_1) transformation is unusual and deserves additional comment, because one could invoke oxidative addition of a silox Me-group to the nominal Nb(III) center followed by olefin insertion in lieu of this single step. First, although structural details are only known for (silox)$_3$Ta(η-CH_2CHEt) (**2**-C_2H_3Et), it is likely that related niobium olefin complexes have a substantial amount of meta-

(86) Cundari, T. R.; Gordon, M. S. *J. Am. Chem. Soc.* **1991**, *113*, 5231−5234.

(87) Calculations at the G3MP2B3 level at 298.15 K give the following: ΔH(S−T, :CMe_2) = −2.7 kcal/mol, ΔH(S−T, :CHEt) = 1.1 kcal/mol, ΔH(S(:CMe_2) − S(:CHEt)) = 8.6 kcal/mol, ΔH(T(:CMe_2) − T(:CHEt)) = 4.8 kcal/mol. Wilcox, C. F., personal communication.

(88) For other unusual abstractions, see: (a) Wada, K.; Pamplin, C. B.; Legzdins, P.; Patrick, B. O.; Tsyba, I.; Bau, R. *J. Am. Chem. Soc.* **2003**, *125*, 7035−7048. (b) Ng, S. H. K.; Adams, C. S.; Hayton, T. W.; Legzdins, P.; Patrick, B. O. *J. Am. Chem. Soc.* **2003**, *125*, 15210−15223.

(89) Chamberlain, L. R.; Kerschner, J. L.; Rothwell, A. P.; Rothwell, I. P.; Huffman, J. C. *J. Am. Chem. Soc.* **1987**, *109*, 6471−6478.

(90) Fryzuk, M. D.; Johnson, S. A.; Rettig, S. J. *J. Am. Chem. Soc.* **2001**, *123*, 1602−1612.

Scheme 7

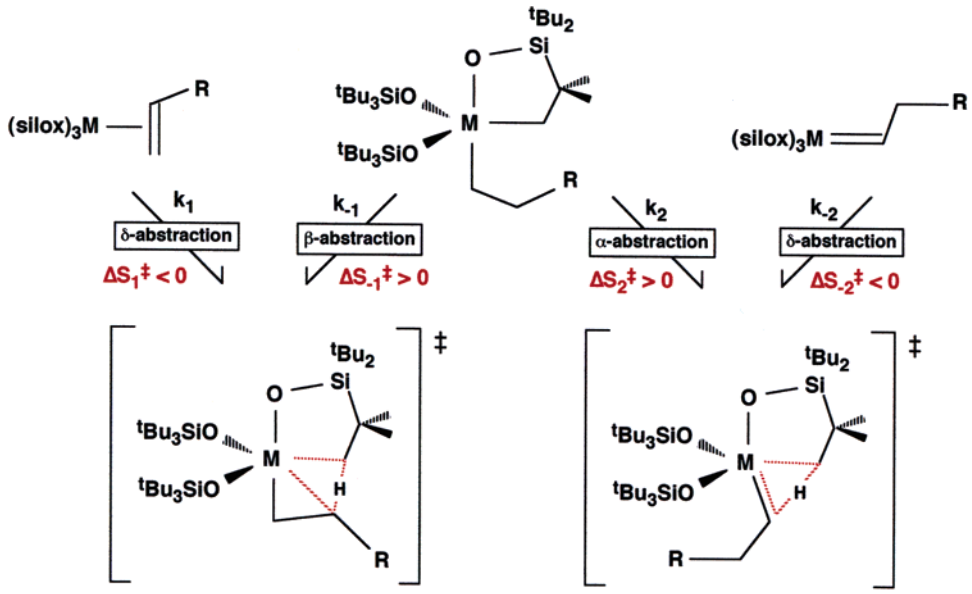

lacyclopropane character;[46,47] that is, that of Nb(V), given the highly reducing nature of the early metal center. Second, it is pertinent to view the overall process from the standpoint of the tuck-in alkyls, (silox)$_2$(R)M(κ^2-O,C-OSi^{t}Bu$_2$CMe$_2$CH$_2$) (M = Nb, **4**−R; M = Ta, **6**-R), partitioning between olefin complex (k_{-1}) and alkylidene formation (k_2). The former process is a β-abstraction (k_{-1}) reaction common to early metal systems, especially those that are hindered, as Buchwald[69,91] and Boncella,[92] among others,[70−73,90] have intimated. The δ-abstraction is simply the microscopic reverse of this well-established process.

Note also the similarity of the transition states for δ-abstraction/β-abstraction and α-abstraction/δ-abstraction (by the alkylidene, k_{-2})[67,68,70,93−96] shown in Scheme 7. α-Abstraction is a common reaction of sterically encumbered early metal centers[22,23] and is distinguished from α-elimination/reductive elimination paths because the latter cannot occur at d^0 metal centers. The KIEs discerned for α-abstraction by the tuck-in alkyls of the 1-butene and norbornene rearrangements are quite comparable to previous cases[63−69] and support the notion that the α-abstraction step (k_2) is rate-determining for the niobium system and for (silox)$_3$Ta(η-^{c}C$_7$H$_{10}$) (**2**-^{c}C$_7$H$_{10}$). Given the similarity in TSs shown in Scheme 7 and the extreme crowding at the metal center that an alternative, six-coordinate, d^0 (silox)$_2$-(olefin)HM(κ^2-O,C-OSi^{t}Bu$_2$CMe$_2$CH$_2$) intermediate would suffer, formation of the tuck-in alkyl (M = Nb, **4**-R; M = Ta, **6**-R) is best construed as occurring via a δ-abstraction by the β-carbon of the olefin on a silox methyl group.

(91) Buchwald, S. L.; Kreutzer, K.; Fisher, R. A. *J. Am. Chem. Soc.* **1990**, *112*, 4600−4601.
(92) (a) Wang, S.-Y. S.; Abbound, K. A.; Boncella, J. M. *J. Am. Chem. Soc.* **1997**, *119*, 11990−11991. (b) Wang, S.-Y. S.; VanderLende, D. D.; Abboud, K. A.; Boncella, J. M. *Organometallics* **1998**, *17*, 2628−2835. (c) Wang, S.-Y. S.; Abboud, K. A.; Boncella, J. M. *Polyhedron* **2004**, *23*, 2733−2749.
(93) Chamberlain, L. R.; Rothwell, I. P.; Huffman, J. C. *J. Am. Chem. Soc.* **1986**, *108*, 1502−1509.
(94) Coles, M. P.; Gibson, V. C.; Clegg, W.; Elsegood, M. R. J.; Porelli, P. A. *J. Chem. Soc., Chem. Commun.* **1996**, 1963−1964.
(95) van der Heijden, H.; Hessen, B. *J. Chem. Soc., Chem. Commun.* **1995**, 145−146.
(96) Vaughan, W. M.; Abboud, K. A.; Boncella, J. M. *J. Am. Chem. Soc.* **1995**, *117*, 11015−11016.

2. Niobium Energetics. Without direct evidence of the intermediate (silox)$_2$(R)M(κ^2-O,C-OSi^{t}Bu$_2$CMe$_2$CH$_2$) (M = Nb, **4**-R), the niobium energetics are limited to assessments of olefin and alkylidene complex ground states and the rate-determining transition state. Figure 4. illustrates the energies of these respective states for each case relative to the energy of (silox)$_3$Nb(η-C$_2$H$_4$) (**1**-C$_2$H$_4$), which is assigned a value of 0.0 kcal/mol. Generally, the rate-determining transition state energies increase as the energies of the ground-state olefin complexes increase, but to a lesser extent. In contrast, the product alkylidenes are relatively similar in energy, with the exceptions of (silox)$_3$Nb=^{c}C$_7$H$_{10}$ (**1**=^{c}C$_7$H$_{10}$) and (silox)$_3$Nb=^{c}C$_6$H$_{10}$ (**1**=^{c}C$_6$H$_{10}$). The ground state of (silox)$_3$Nb(η-^{c}C$_6$H$_{10}$) (**1**-^{c}C$_6$H$_{10}$) is given a value of >8.4 kcal/mol, and this inequality is designated by an arrow in Figure 4, as is the transition state for rearrangement because the $\Delta G_f^{\ddagger}$ of 29.5 kcal/mol is fixed. The magnitudes of the niobium rearrangement activation energies are substantial and indicate that even with an internal "catalyst", the cyclometalating silox ligand, the conversion of olefin to alkylidene in the absence of Brønsted or Lewis acids is energetically costly.

The gross features of Figure 4 suggest a linear free energy (LFE) relationship for the rearrangement. Given the accuracy of the calculations in assessing relative ground-state olefin complex energies, (silox)$_3$Nb(η-^{c}C$_6$H$_{10}$) (**1**-^{c}C$_6$H$_{10}$) was assigned the calculated value of 10.9 kcal/mol. Figure 5 illustrates two related LFEs: $\Delta\Delta G_f^{\ddagger} = \alpha - \beta\Delta\Delta G°$(**1**-ole) and $\Delta\Delta G_f^{\ddagger} = \alpha' + \beta'\Delta\Delta G°$(**1**=alk/**1**-ole). As espoused above, the activation energies for rearrangement are highly dependent on the ground-state energy of (silox)$_3$Nb(ole) (**1**-ole), with $\beta = 0.56$ ($R^2 = 0.74$) for the entire set of substrates, and $\beta = 0.59$ ($R^2 = 0.93$) with the outlying norbornene point removed. The norbornene is certainly a unique case. While it is tempting to place it in a class with the other cyclics, **1**-^{c}C$_7$H$_{10}$ is 3.2 and ~6.9 kcal/mol lower than the cyclopentene and cyclohexene complexes, respectively, an observation consistent with its greater relief of ring strain[84,85] upon binding. Note that its $\Delta G_f^{\ddagger}$ is quite similar to the other cyclics, rendering it an outlying point because the ground state of **1**-^{c}C$_7$H$_{10}$ is roughly 4 kcal/mol

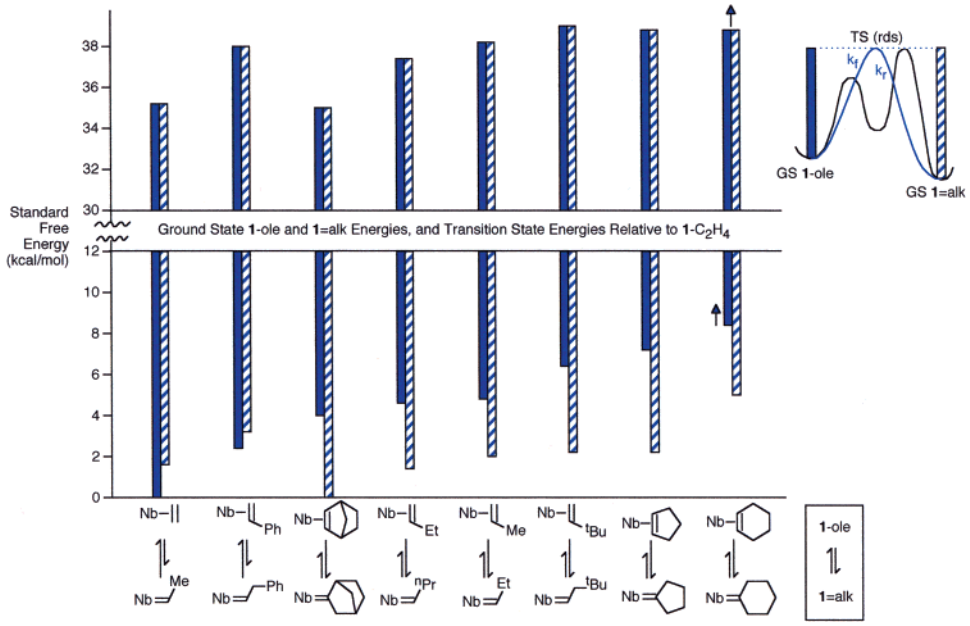

Figure 4. Relative standard free energies (kcal/mol, 103 °C) of $(silox)_3Nb(ole)$ (**1**-ole) indicated by bottom of solid blue column and those of $(silox)_3Nb(alk)$ (**1**=alk) indicated by bottom of striped blue column. The solid blue column is the activation free energy for the overall forward step in the rearrangement, $\Delta G_f^{\ddagger}$, while the striped blue column refers to $\Delta G_r^{\ddagger}$. The common top of the columns refers to the transition state energy of the rate-determining step. All energies are relative to $(silox)_3Nb(\eta\text{-}C_2H_4)$ (**1**-C_2H_4) at 0.0 kcal/mol. The arrows indicate that the columns represent lower limits for the ground state of $(silox)_3Nb(\eta\text{-}^cC_6H_{10})$ (**1**-$^cC_6H_{10}$) and its accompanying transition state.

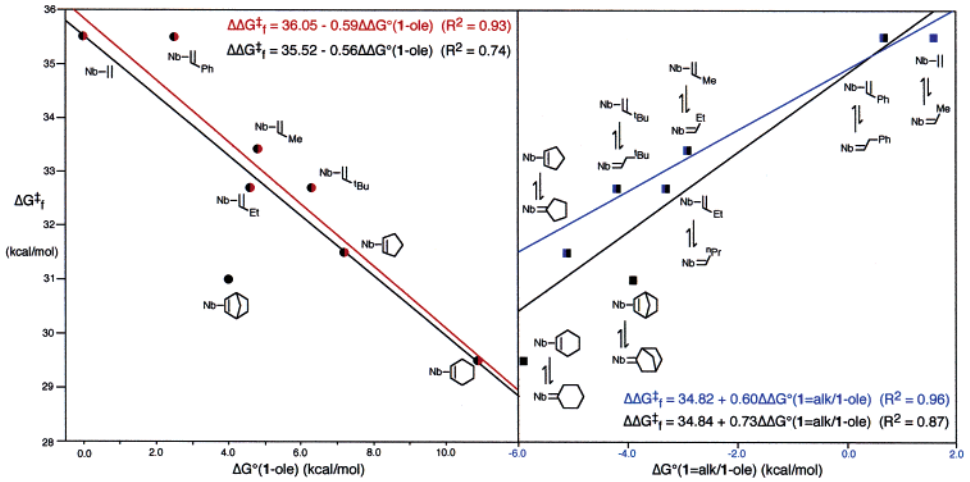

Figure 5. Linear free energy relationships: (1) the relation of the $\Delta G_f^{\ddagger}$'s for the $(silox)_3Nb(ole)$ (**1**-ole) to $(silox)_3Nb(alk)$ (**1**=alk) conversion to the relative standard free energies of **1**-ole given as $\Delta\Delta G_f^{\ddagger} = \alpha - \beta\Delta\Delta G°$(**1**-ole); (2) the relation of the $\Delta G_f^{\ddagger}$'s to the standard free energy change of the **1**-ole to **1**=alk conversion given as $\Delta\Delta G_f^{\ddagger} = \alpha' + \beta'\Delta\Delta G°$(**1**=alk/**1**-ole). The red line has the $(silox)_3Nb(\eta\text{-}^cC_7H_{10})$ (**1**-$^cC_7H_{10}$) point removed, and the blue line has the **1**-$^cC_7H_{10}$ and $(silox)_3Nb(\eta\text{-}^cC_6H_{10})$ (**1**-$^cC_6H_{10}$) points left out. The calculated $\Delta G°$(**1**-$^cC_6H_{10}$) of 10.9 kcal/mol was used, but it is likely to approach 13.6 kcal/mol. See text for explanation.

lower. The styrene case, while not dropped in either LFE, appears to have a slightly higher than expected $\Delta G_f^{\ddagger}$ or higher $\Delta G°$(**1**-C_2H_3Ph). Since it is bulkier than other monosubstituted olefins, yet binds more strongly, the latter is unlikely. In the conversion to the transient $(silox)_2(PhCH_2CH_2)Nb(\kappa^2\text{-O,C-OSi}^t\text{Bu}_2CMe_2CH_2)$ (**4**-CH_2CH_2Ph) complex, it is the β-carbon−niobium bond that is broken, yet this is the olefin carbon containing the inductively withdrawing Ph group.[75,76] It is likely that this TS is achieved via an elongated reaction coordinate, i.e., the d(Nb−C_β(Ph)) is shorter than comparative d(Nb−C_β-(R)), leading to a higher energy transition state (vide infra). For this feature to impact Figure 4, the styrene rearrangement may be the only case in which tuck-in alkyl formation is rate-determining.

The second LFE relationship correlates $\Delta G_f^{\ddagger}$ with the standard free energy change of the reaction, $\Delta G°$(**1**=alk/**1**-ole), a more conventional comparison that yields a β of 0.73 ($R^2 = 0.87$). In viewing this correlation, the cyclohexene and norbornene cases are moderately outlying, and when removed a β of 0.60 ($R^2 = 0.96$) is obtained. As stated above, the $\Delta G°$(**1**-$^cC_7H_{10}$) is anomalously low, presumably because of relief of ring strain, and the norbornylidene **1**=$^cC_7H_{10}$ is only modestly lower in energy than the remaining alkylidenes (~2 kcal/mol); as such the $\Delta G°$(**1**-$^cC_7H_{10}$/**1**=$^cC_7H_{10}$) in this case is higher than expected. Ring strain is also relieved in formation of the norbornylidene,[84,85] but it is difficult to estimate the extent to which the sterics of this largest substrate offset this factor. For cyclohexene, it is unlikely that the slight displacement from the

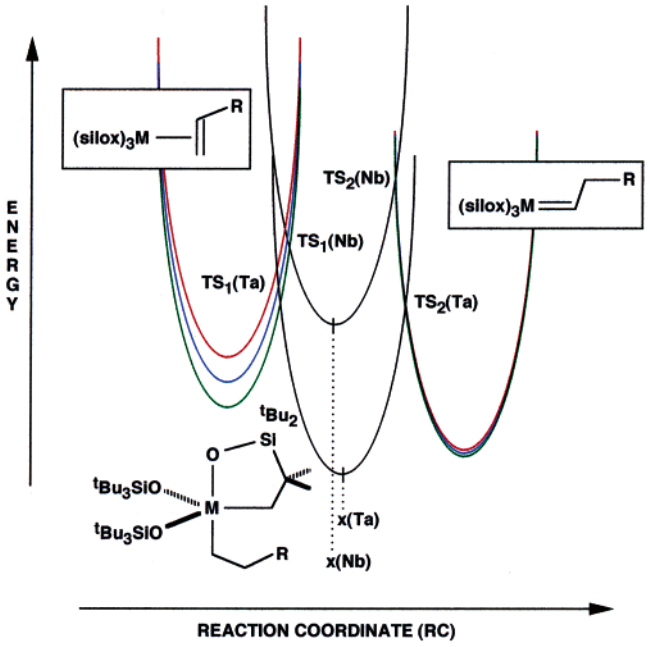

Figure 6. General reaction coordinate vs energy diagram for the (silox)$_3$M(ole) (M = Nb, **1**-ole; Ta, **2**-ole) to (silox)$_2$RM(κ^2-O,C-OSi^{t}Bu$_2$CMe$_2$CH$_2$) (M = Nb, **4**-R; Ta, **6**-R) to (silox)$_3$M(alk) (M = Nb, **1**=alk; Ta, **2**=alk). The Ta and Nb olefin and alkylidene complexes are portrayed with the same energy surfaces *for convenience*, and are not meant to imply they exist at the same absolute energies.

remaining cases is due to its $\Delta G_f^{\ddagger}$ or $\Delta G°$(**1**-^{c}C$_6$H$_{10}$), because the previous correlation was excellent. Cyclohexylidene **1**=^{c}C$_6$H$_{10}$ is not as low in energy as the remaining alkylidenes, and while this could be the origin of the displacement from the line, it is more likely that the $\Delta G°$ for this case is still undervalued at −5.9 kcal/mol and might be as much as −8.6 if the calculated values are corrected as rationalized above.

The LFE relationship is consistent with the proposed tuck-in alkyl to alkylidene transformation as the rate-determining step, as Figure 6 illustrates. Electronic differences in the olefin should not have substantial impact on the energies of (silox)$_2$RNb(κ^2-O,C-OSi^{t}Bu$_2$CMe$_2$CH$_2$) (**4**-R) or the alkylidenes (silox)$_3$Nb=(alk) (**1**=alk); hence the transition state connecting these two species should also be relatively free of the influence of olefin substituents. The olefin complexes are sensitive to electronic changes, and the transition states connecting them to the tuck-in alkyl, **4**-R, should also be influenced by similar amounts of energy. If this first transition state were rate-determining, then β would be quite small. Its magnitude is far more consistent with a rate-determining second transition state. As the energies of **1**-ole change, energies of the transition state linking **4**-R to **1**=alk are relatively insensitive, permitting a substantial fraction of $\Delta\Delta G°$(**1**-ole) to be transposed to $\Delta\Delta G_f^{\ddagger}$. A destabilization of the olefin complex ground state leads to swifter rates of rearrangement. Activation energies ($\Delta G_r^{\ddagger}$'s) of the reverse rearrangement should also be less sensitive to substituent. Table 4 reveals that this is the case, with $\Delta G_r^{\ddagger}$ (ave) = 35.6 (10) kcal/mol representing a modest range of 33.9−36.9 kcal/mol (34.8−36.9 with the ethylene case excluded) compared to $\Delta G_f^{\ddagger}$ (ave) = 32.7 (21) with its much greater range of 29.5−35.5 kcal/mol.

3. Tantalum Energetics. While the essentials of the niobium system are understood, the energetics of the tantalum rearrangements pose several problems: (1) since the olefin complexes cannot be equilibrated, the relative energies of the species must be estimated, (2) the tuck-in alkyls, (silox)$_2$RTa(κ^2-O,C-OSi^{t}Bu$_2$CMe$_2$CH$_2$) (**6**-R), are typically the most stable species and dominate the energetics, and (3) **6**-R and the product alkylidene (silox)$_3$Ta=alk (**2**=alk) are often so stable that the relative energy of corresponding olefin complex (silox)$_3$Ta(ole) (**2**-ole) cannot be discerned.

Since the calculated energies of (HO)$_3$Nb(ole) (**1′**-ole) closely matched the experimental values of (silox)$_3$Nb(ole) (**1**-ole), a reasonable amount of confidence can be placed on the corresponding tantalum olefin complex energies. Figure 7 illustrates the relative energies of all ground states and transition states in the tantalum system referenced to (silox)$_3$Ta(η-C$_2$H$_4$) (**2**-C$_2$H$_4$) at 0.0 kcal/mol; **2**-ole is arranged according to the calculated relative energies of (HO)$_3$Ta(ole) (**2′**-ole). Note that the rearrangements of the propene, 1-butene, and cyclohexene complexes are undetermined because **2**-ole cannot be observed at equilibrium. In regard to these specific cases, energies pertaining to the **2**=alk, **6**-R, and their connecting transition states are indicated as maxima in the graph through labeling with arrows.

Figure 7 shows that the tuck-in alkyls, (silox)$_2$RTa(κ^2-O,C-OSi^{t}Bu$_2$CMe$_2$CH$_2$) (**6**-R), are the most stable species for the acyclic olefin cases. For norbornene, **6**-^{c}C$_7$H$_{11}$ is not observed, and for cyclopentene and cyclohexene, the **6**-^{c}C$_5$H$_9$ and **6**-^{c}C$_6$H$_{11}$ complexes are 1.0 and 0.6 kcal/mol above their respective alkylidenes **2**=^{c}C$_5$H$_9$ and **2**=^{c}C$_6$H$_{11}$. Secondary alkyl **6**-R species are expected to be higher in energy than primary alkyl **6**-R derivatives on the basis of electronic effects. Studies of (silox)$_2$(^{t}Bu$_3$SiNH)Ti−R suggest that a 1.3−2.6 kcal/mol difference is plausible.[75] In addition, they should have the most severe steric interactions of any cyclometalated intermediates. The tuck-in primary alkyls (**6**-R, R = Et, CH$_2$CH$_2$Ph, ^{n}Pr, ^{n}Bu) are about 2.0−2.5 kcal/mol more stable than their respective alkylidenes; hence the increase in energy of tuck-in secondary alkyls is roughly 3 kcal/mol. A similar steric penalty for secondary alkylidenes might contribute to their higher energy in relation to their more stable primary counterparts and **6**-R (Ta).

As Figure 7 shows, by dominating the energetics, the tuck-in alkyls (silox)$_2$RTa(OSi^{t}Bu$_2$C-Me$_2$CH$_2$) (**6**-R) change the importance of the two transition states relative to the niobium rearrangements. The α-abstraction (k_2) step of the (silox)$_3$Ta(η-C$_2$H$_4$) (**2**-C$_2$H$_4$) rearrangement is the slowest, and the second transition state linking **6**-Et and (silox)$_3$Ta=CHMe (**2**=CHMe) is clearly the highest. In the norbornene case, the KIE for the overall rearrangement of **2**-^{c}C$_7$H$_{10}$ to **2**=^{c}C$_7$H$_{10}$ is best accounted for in terms of a rate-determining k_2 step, just as in all the niobium cases. However, it appears that in the remaining tantalum rearrangements, the first transition state linking **2**-ole to **6**-R is the highest because of the influence of $\Delta G°$(**6**-R). For the sake of argument, assume the $\Delta G°$ for **2**-ole ⇌ **2**=alk is the same as that in the corresponding niobium cases. In support, the calculated $\Delta G°$(**2′**-ole/**2′**-alk) values were effectively the same for niobium and tantalum. In certain cases where ambiguities exist (propene, 1-butene), **6**-^{n}Pr, **6**-^{n}Bu, **2**=CHEt, and **2**=CH^{n}Pr can be assigned relative standard free energies of −0.4, −0.7, 1.7, and 1.3 kcal/mol in place of the arrows in Figure 7. As a consequence, the transition states for **6**-^{n}Pr ⇌ **2**=CHEt and **6**-^{n}Bu ⇌ **2**=CH^{n}Pr are at $\Delta G°$ = 32.1 and 31.9 kcal/mol.

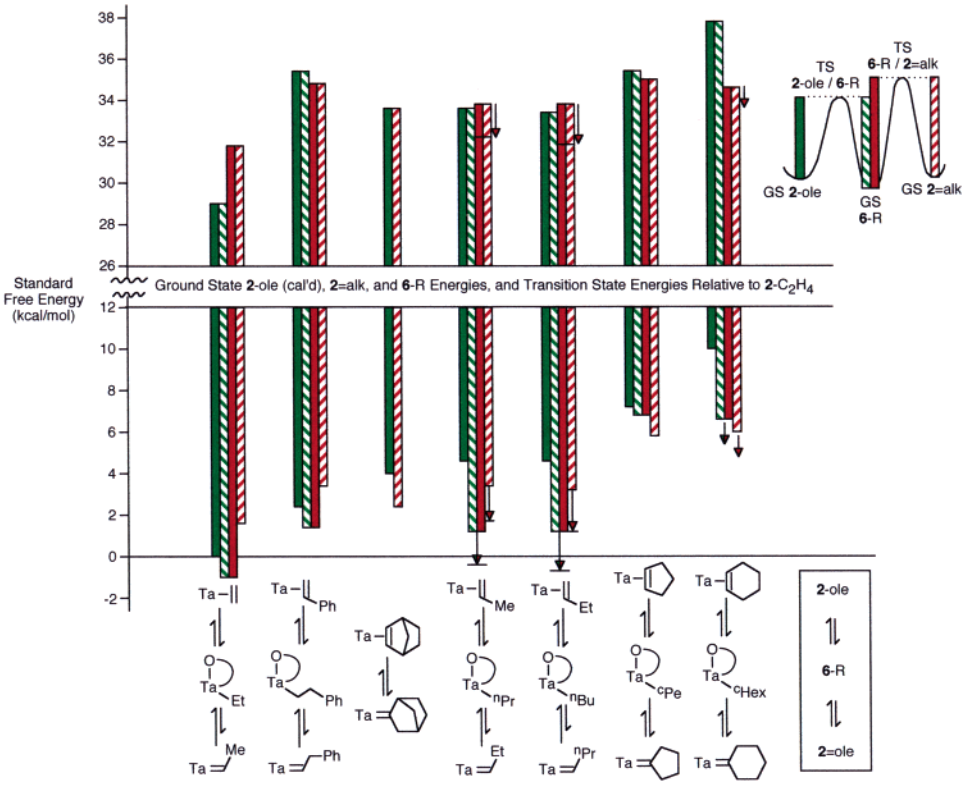

Figure 7. Relative standard free energies (kcal/mol, 103 °C) of $(silox)_3Ta(ole)$ (**2**-ole) indicated by bottom of solid green column and those of $(silox)_3Ta(alk)$ (**2**═alk) indicated by bottom of striped red column. The common bottom of the striped green and solid red columns indicates the relative $\Delta G°$ of $(silox)_2RTa(\kappa^2\text{-O,C-OSi}^t\text{Bu}_2\text{CMe}_2\text{CH}_2)$ (**6**-R). The solid red, red-striped, green, and green-striped columns represent the activation free energies associated with k_1, k_{-1}, k_2, and k_{-2} of Scheme 7, respectively. The top of the two green columns is the relative standard free energy of the transition state for **2**-ole to **6**-R, and the top of the red columns is the $\Delta G°$ of the transition state for **6**-R to **2**═alk. All energies are relative to $(silox)_3Ta(\eta\text{-}C_2H_4)$ (**2**-C_2H_4) at 0.0 kcal/mol, and the relative **2**-ole energies are taken from computations. The arrows indicate that the respective state energies are maxima, and the bars below the arrows indicate estimates of their probable values. See text for explanation.

Now in every case, save ethylene and norbornene, the second transition state is *lower* than the first, despite $\Delta G_2^{\ddagger}$ being *greater* than $\Delta G_1^{\ddagger}$ in every remaining case except cyclopentene.

It is the influence of $\Delta G°((silox)_2RTa(\kappa^2\text{-O,C-OSi}^t\text{Bu}_2\text{CMe}_2\text{-CH}_2)$ (**6**-R)) and its reaction coordinate relative to $(silox)_3$-Ta(ole) (**2**-ole) and $(silox)_3Ta(alk)$ (**2**═alk) that are responsible for the more rapid reaction rates in the tantalum system and the corresponding transition state energy changes. Figure 6 provides a rough illustration of the energetics of the olefin to alkylidene rearrangement, with the caveat that niobium and tantalum have been placed on the same diagram only as a matter of convenience. A natural consequence of the high energy position of $(silox)_2RNb(\kappa^2\text{-O,C-OSi}^t\text{Bu}_2\text{CMe}_2\text{CH}_2)$ (**4**-R) is that variation of $(silox)_3Nb(ole)$ (**1**-ole) ground-state energies results in dramatic rearrangement rate changes because TS_2 is rate-determining. The significant stabilization of **6**-R relative to its niobium congener does not explain why TS_2 is typically lower in energy than TS_1 in most tantalum cases. The change in reaction coordinate for **6**-R shown in Figure 6 must accompany its energetic change relative to niobium to rationalize this observation.

From the standpoint of energies, the greater importance of the tuck-in alkyl intermediate to the tantalum system may be due to the true M(V) character of this intermediate. The olefin and alkylidene species can be considered M(III)— understanding the olefin complex certainly has metalacyclopropane character and alkylidenes are usually treated as dianionic—and hence a greater propensity toward the higher oxidation state should lie toward the third-row metal. Likewise, the second-row niobium should accommodate the pseudo-lower oxidation states of **1**-ole and **1**═alk better than the tantalum congeners. The shift in reaction coordinate relative to **2**-ole and **2**═alk that accompanies the energy lowering of **6**-R relative to its niobium counterpart is difficult to comment about. It is plausible that tantalum alkylidene species are more "M(V)-like" than niobium alkylidene complexes, and that geometry changes favoring a more compressed RC along the **6**-R to **2**═alk trajectory reflect that, but absent substantial structural data this must remain speculation. Because of the complicated nature of **6**-R, no attempt to model its energetics by quantum calculations was made.

Figure 6 can be used to generalize the tantalum system as much as possible. It is expected that much of the energy differences in the ground states of $(silox)_3Ta(ole)$ (**2**-ole) translate to TS_1, because the metal olefin interaction is being disrupted in this transition state. The activation free energies corresponding to k_1 should not vary a great deal, and $\Delta G_1^{\ddagger}(ave) = 29.3(16)$ kcal/mol; with $\Delta G_1^{\ddagger}$(**2**-CH_2CH_2Ph) removed, even less variation is noted (28.7(6) kcal/mol). Likewise, the spread in $\Delta G^{\ddagger}_1$ (without the outlying styrene case) is only 1.7 kcal/mol. There is essentially no LFE relationship between $\Delta G_1^{\ddagger}$ and $\Delta G°$(**6**-R/**2**-ole); for $\Delta\Delta G_1^{\ddagger} = \beta\Delta\Delta G°$(**6**-R/**2**-ole) + c_1, $\beta < 0.2$ with or without inclusion of data pertaining to **2**-CH_2CH_2Ph, and the correlation coefficients are <0.1 in both cases.

Greater variation in activation free energies would be expected for k_{-1}, since it is unlikely that variation in tuck-in alkyl energies would be as strongly coupled to the olefin-like transition state

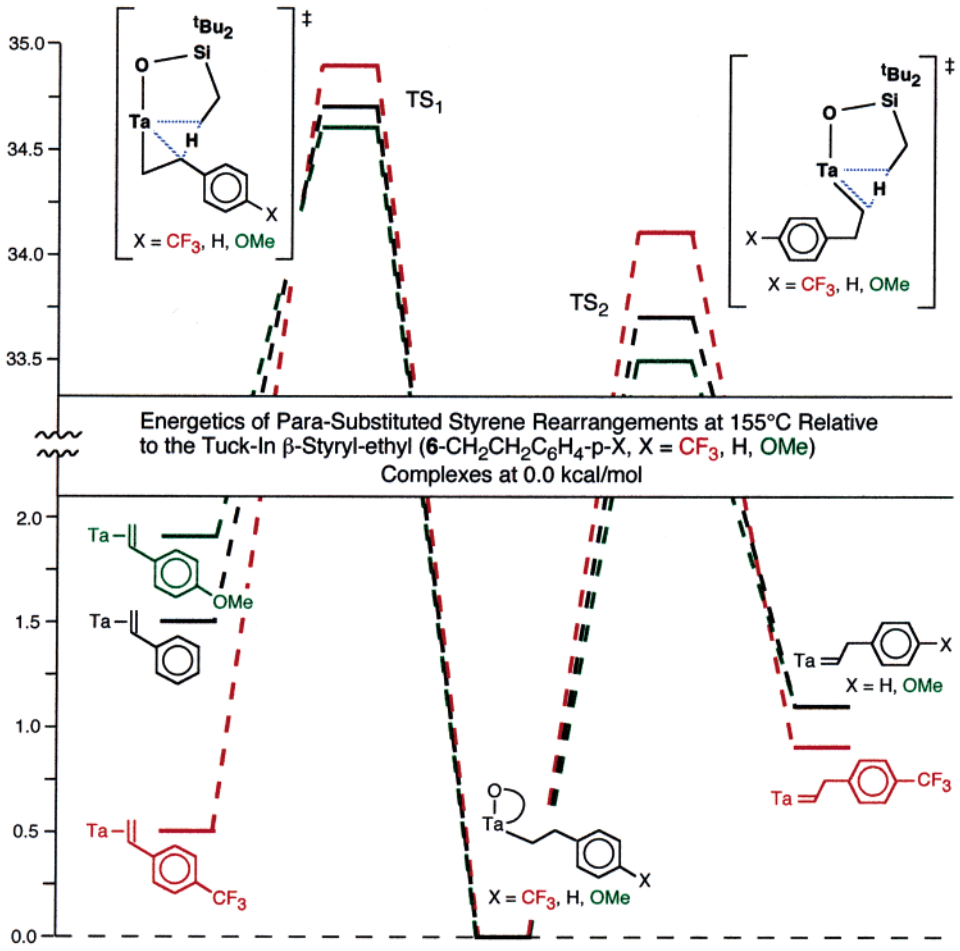

Figure 8. Relative standard free energies (kcal/mol, 155 °C) of (silox)$_3$Ta(η-C$_2$H$_3$C$_6$H$_4$-*p*-X) (**2**-C$_2$H$_3$C$_6$H$_4$-*p*-X, X = CF$_3$ (red), H (black), OMe (green)), (silox)$_2$(X-*p*-C6H4CH2CH2)Ta(κ^2-O,C-OSi^{t}Bu$_2$CMe$_2$CH$_2$) (**6**-C$_2$H$_4$C$_6$H$_4$-*p*-X, X = CF$_3$, H, OMe), and (silox)$_3$Ta=CHCH$_2$C$_6$H$_4$-*p*-X (**2**-C$_2$H$_3$C$_6$H$_4$-*p*-X, X = CF$_3$, H, OMe). Activation energies for k_1, k_{-1}, k_2, and k_3 of Scheme 7 are indicated by red (X = CF$_3$), black (X = H), and green (X = OMe) dashed lines. The tuck-in alkyls **6**-C$_2$H$_4$C$_6$H$_4$-*p*-X have been arbitrarily placed at 0.0 kcal/mol, and all ground and transition state energies are given relative to this reference state. See text for rationale.

TS$_1$. For the following arguments, $\Delta G°$(**6**-R) values are estimated on the basis of the assumption that **2**-ole $\rightleftharpoons$ **2**=alk is the same as that in the corresponding niobium cases as explained above (the maximum $\Delta G_{-1}^{\ddagger}$ of **6**-^{c}C$_7$H$_{11}$ is estimated to be 27.8 kcal/mol; this corresponds to $\Delta G°$(**6**-^{c}C$_7$H$_{11}$) being at least 3.4 kcal/mol greater than $\Delta G°$(**2**=^{c}C$_7$H$_{10}$)). With the obviously outlying styrene data removed, $\Delta\Delta G_{-1}^{\ddagger} = \beta\Delta\Delta G°$(**2**-ole/**6**-R) + c_{-1} and $\beta < 0.94$ with a correlation coefficient of $R^2 = 0.97$. A correspondingly large $\Delta G_{-1}^{\ddagger}$(ave) of 31.3(27) kcal/mol is observed along with a range of $\Delta G_{-1}^{\ddagger}$'s of 6.3 kcal/mol. It is not surprising that **2**-CH$_2$CH$_2$Ph and its TS$_1$ are an oddity in this assessment. Recall that reversible cyclometalation into the α-position of the bound styrene was suspected from the labeling studies, and it is postulated that the inductively withdrawing phenyl substituent renders the olefin more strongly bound than other acylic olefins. As espoused for the niobium−styrene case, the reaction coordinate should be correspondingly elongated and TS$_1$ should be higher in energy than other acyclic cases.

While LFE relationships appear to be present for $\Delta G_2^{\ddagger}$ and $\Delta G_{-2}^{\ddagger}$, a close inspection revealed that the data are bunched in acyclic and cyclic groupings and the fits are inappropriate. Figure 6 suggests that for like species, the activation free energies leading to the second transition state, TS$_2$, should be similar. For the acyclic cases, $\Delta G_2^{\ddagger}$(ave, acyclic) = 32.8(4) kcal/mol and $\Delta G_{-2}^{\ddagger}$(ave, acyclic) = 30.6(5) kcal/mol, with corresponding ranges of 0.8 and 0.9 kcal/mol, respectively. The cyclic cases display a $\Delta G_2^{\ddagger}$(ave, cyclic) of 28.0(2) kcal/mol with a small range (≤0.3 kcal/mol), but possess a more scattered array of $G_{-2}^{\ddagger}$ values (29.6(14) kcal/mol) with a large range (2.6 kcal/mol). This discrepancy from the view in Figure 6 is due to the norbornene case, in which $\Delta G°$(**6**-^{c}C$_7$H$_{11}$) is estimated.

As Scheme 7 shows, the transition from olefin complex to tuck-in alkyl requires elongations of *d*(Ta−C$_\beta$) and *d*(silox methyl C−H) as new Ta−C (from cyclometalation) and C$_\beta$H bonds form. The reaction coordinate has a similar complexity in the transition from tuck-in alkyl to alkylidene. The role the reaction coordinate plays in distinguishing the energetics of the various substrates of this study is difficult to understand without structural information, but electronic factors determined in the para-substituted styrene derivatives can provide some insight. Figure 8 illustrates the energetics of (silox)$_3$Ta(η-C$_2$H$_3$Ph-*p*-X) (X = OMe, **2**-C$_2$H$_3$Ph-*p*-OMe; H, **2**-C$_2$H$_3$Ph; CF$_3$, **2**-C$_2$H$_3$Ph-*p*-CF$_3$) and their conversions to (silox)$_2$(X-*p*-PhCH$_2$CH$_2$)Ta(κ^2-O,C-OSi^{t}Bu$_2$CMe$_2$CH$_2$) (X = OMe, **6**-C$_2$H$_4$Ph-*p*-OMe; H, **6**-C$_2$H$_4$Ph; CF$_3$, **6**-C$_2$H$_4$Ph-*p*-CF$_3$) and (silox)$_3$Ta=CHCH$_2$Ph-*p*-X (X = OMe, **2**=CHCH$_2$Ph-*p*-OMe; H, **2**=CHCH$_2$Ph; CF$_3$, **2**=CHCH$_2$Ph-*p*-CF$_3$). The diagram is referenced to the three **6**-R species at 0.0 kcal/mol at the same position along the

reaction coordinate. There is a modest check on this assumption via some corresponding niobium equilibria. As Table 3 shows, the $\Delta G_{103}°$(**1**-C_2H_3Ph-*p*-OMe/**1**-C_2H_3Ph) value is 0.55 kcal/mol, close to the 0.4 kcal/mol for the tantalum equilibrium based on **6**-R as the reference state. In addition, the $\Delta G_{103}°$(**1**-C_2H_3Ph-*p*-CF_3/**1**-C_2H_3Ph) value is −1.22 kcal/mol, and Figure 8 shows the related tantalum equilibrium to be −1.0 kcal/mol.

Note that the biggest spread in energies corresponds to the ground states of **2**-C_2H_3Ph-*p*-X. If the reaction coordinates for all X's were the same, the TS_1's for the X = CF_3, H, and OMe cases would be in that order, but they are reversed. The highest energy olefin complex, **2**-C_2H_3Ph-*p*-OMe, possesses the lowest energy TS_1. The reaction coordinate for the conversion of **2**-C_2H_3Ph-*p*-OMe to **6**-C_2H_4Ph-*p*-OMe must be compressed relative the X = H, which in turn is compressed relative to X = CF_3. While structural evidence is not available, one would expect the *d*(TaC) of the more withdrawing CF_3-substituted styrene to be shorter, followed by X = H and finally X = OMe. This would correspond to a lengthening of the RC for X = CF_3 etc. A compression of the RC for X = H, OMe is also seen in the **6**-C_2H_4Ph-*p*-X to **2**=$CHCH_2$Ph-*p*-X conversion through TS_2, although here the effect is less easily rationalized. With $\Delta G°$(**6**-C_2H_4Ph-*p*-X) serving as the reference state, the fact that $\Delta G°$(**2**=$CHCH_2$Ph-*p*-X) manifests little difference makes sense because the para-substituents are not electronically coupled to the metal. On the basis of Figure 6, minimal TS_2 energy differences are expected, and only an ∼0.8 kcal/mol range is observed, but the substituents are reversed, and while a compression in RC can explain this, its origin is not especially transparent.

One oddity that deserves comment is the $\Delta G°$(**2**-$^cC_5H_8$ ⇌ **2**=$^cC_5H_8$) of −1.3 kcal/mol in comparison to the −5.1 kcal/mol observed for $\Delta G°$(**1**-$^cC_5H_8$ ⇌ **1**=$^cC_5H_8$). Given the near size equivalence of niobium and tantalum (r_{cov} = 1.34 Å), these reproducible results are difficult to interpret. While not as large a difference, the $\Delta G°$(**2**-$^cC_7H_{10}$ ⇌ **2**=$^cC_7H_{10}$) of −1.7 kcal/mol is also distinctly less than its niobium counterpart, $\Delta G°$-(**1**-$^cC_7H_{10}$ ⇌ **1**=$^cC_7H_{10}$), which has a value of −3.9 kcal/mol. These disparate energies between second- and third-row species hint at an unusual electronic origin. Since the metal alkylidene bonds of the norbornene and cyclopentene species contain a greater degree of s-character due to the modest ring strain in these compounds, it is conceivable that subtleties in the overlap and energies of the d_{z^2} orbitals of Nb and Ta may manifest themselves here. It has been shown calculationally that the d_{z^2} orbital of $(HO)_3$Ta (**2′**) is substantially lower than the corresponding niobium orbital,[38] and this is, in part, what is responsible for the dramatic stability and reactivity of $(silox)_3$Ta (**2**)[39] relative to its nonisolable counterpart, $(silox)_3$Nb (**1**).

In summary, as in the niobium system, the ground-state energies of the olefin complexes, $(silox)_3$Ta(ole) (**2**-ole), play a major role in affecting the energies of TS_1. This step is isolated for all substrates except norbornene, and very modest changes in rate are found for the formation of the tuck-in alkyls, $(silox)_2$RTa($OSi^tBu_2CMe_2CH_2$) (**6**-R), which is consistent with the view in Figure 6. The energy and position along the reaction coordinate of **6**-R change the nature of the rearrangement for tantalum. Relative to **2**-ole and **2**=alk, **6**-R is more stable in the acyclic cases,[75] although **2**-ole ⇌ **2**=alk is probably very similar to that of the niobium system, at least according to a few direct measurements and calculated relative energies. For the cyclics, **6**-R is stable enough to be observable except for **6**-$^cC_7H_{11}$, which is presumed to have steric interactions (Ta−C(sp^3)) that are more severe than **2**=$^cC_7H_{10}$ (Ta−C(sp^2)).

Conclusions

Although the group 5 complexes above lack the space necessary to do productive olefin metathesis chemistry, they are representative of the class of compounds used as catalysts. In these systems, metal alkylidenes that possess *β*-hydrogens are not only kinetically stable, but also are most often more thermodynamically stable than their olefin isomers. While this contradicts some studies pertaining to later transition metals, energetic differences between isomeric alkylidene and olefin complexes are likely to be minimal. From a mechanistic standpoint, the isomerization process required a substantial amount of activation energy in every case, and each was studied in nonpolar, aprotic media because of the sensitivity of the compounds. Even though the siloxide ligand mediated the reversible olefin to alkylidene rearrangements, a great deal of reorganization energy was expended to form the cyclometalated intermediate. It can be concluded on the basis of these studies that *β*-hydrogen-substituted alkylidenes are thermodynamically *and* kinetically quite stable. However, one can imagine that alkylidene complexes that are stable to a variety of functional groups, including those of polar and protic solvents, may be subject to a number of isomerization pathways (e.g., L_nM=$CR(CH_2R')$ + H^+ ⇌ $[L_nM-CRH(CH_2R')]^+$ ⇌ $L_nM(RHC$=$CHR')$ + H^+) that do not have energy requirements of large magnitude. In such instances, it may be the thermodynamic stability of the alkylidenes that renders them catalytically active under conditions where isomerization could severely inhibit catalysis.

Finally, many olefin metathesis catalysts are generated in situ via the combination of a high oxidation state complex, typically a d^0 metal halide, and a compound that can serve as an alkylating agent (e.g., $MX_n + 2/m\ R_mM' \rightarrow X_{n-2}MR_2 + 2/m\ X_mM'$).[17,18] Following alkylation, α-abstraction can then lead to an alkylidene (e.g., $X_{n-2}MR_2 \rightarrow X_{n-2}M$=$CHR' + RH$) that is competent for metathesis. An alternative pathway is suggested by these investigations, whereby the high oxidation state transition metal complex (MX_n) is reduced by the main group $M'R_m$ species. The lower valent compound may capture an olefin, and its subsequent rearrangement to an alkylidene then engenders metathesis.

Experimental Section

General Considerations. For a detailed experimental, see the Supporting Information. All manipulations were performed using either glovebox or high vacuum line techniques. All glassware was oven-dried, NMR tubes for sealed tube experiments were flame-dried under vacuum, all solvents were scrupulously dried and degassed, and all gases were dried. $(silox)_3$Ta (**1**-Ta),[40] $(silox)_2$HTa(κ^2-O,C-$OSi^tBu_2CMe_2CH_2$) (**8**),[42] $(silox)_3$Ta(η-H_2CCHR) (R = H, **2**-C_2H_4; Me, **2**-C_2H_3Me),[42] $(silox)_3$Nb(4-pic) (**1**-4-pic),[37,38] $(silox)_3$Nb(η-H_2CCHPh) (**1**-C_2H_3Ph),[37] $(silox)_3NbPMe_3$ (**1**-PMe_3),[38] *β*,*β*-dideuteriostyrene,[77] 2,3-dideuterionorbornene,[78−80] and 1,2-dideuteriocyclohexene[83] were prepared by literature procedures.

Procedures. 1. $(silox)_3NbCl_2$ (3). Into a 100-mL glass bomb charged with $NbCl_5$ (4.49 g, 16.62 mmol) and Na(silox)[97] (12.10 g, 50.75 mmol,

(97) Covert, K. J.; Wolczanski, P. T.; Hill, S. A.; Krusic, P. J. *Inorg. Chem.* **1992**, *31*, 66−78.

3.05 equiv) 20 mL of toluene was distilled at −78 °C. The bomb was sealed and heated to 100 °C for 10 d, giving a pale yellow-green slurry. Upon filtration, crystallization from THF at −78 °C yielded 11.85 g of colorless **3** in two crops (75%). Anal. Calcd for $C_{36}H_{81}Si_3O_3NbCl_2$: C, 53.38; H, 10.08. Found: C, 53.29; H, 10.30.

2. (silox)$_3$Nb(ole) (1-ole) from (silox)$_3$Nb(4-pic) (1-4-pic). A 50-mL bomb reactor was charged with (silox)$_3$Nb(4-pic) (**1**-4-pic), the system was evacuated, and 10 mL of benzene was transferred. The gaseous reagent (∼5 equiv) was condensed into the bomb at 77 K from a calibrated gas bulb. The reaction mixture was stirred for variable times and temperatures, transferred to a flask, and crystallized. **a. (silox)$_3$Nb(η-C_2H_4) (1-C_2H_4).** After a 30-min reaction time at 23 °C, isolation from diethyl ether yielded 333 mg of **1**-C_2H_4 as dark green microcrystals (92%). **b. (silox)$_3$Nb(η-C_2H_3Me) (1-C_2H_3Me).** After a 30-min reaction time at 23 °C, isolation from diethyl ether yielded 250 mg of **1**-C_2H_3Me as dark green microcrystals (67%). Anal. Calcd for $C_{39}H_{87}Si_3O_3Nb$: C, 59.96; H, 11.22. Found: C, 59.20; H, 10.89. **c. (silox)$_3$Nb(η-C_2H_3Et) (1-C_2H_3Et).** After a 30-min reaction time at 23 °C, isolation from diethyl ether yielded 385 mg of **1**-C_2H_3Et as dark green microcrystals (81%). Anal. Calcd for $C_{40}H_{89}Si_3O_3Nb$: C, 60.41; H, 11.28. Found: C, 60.25; H, 11.34. **d. (silox)$_3$Nb(η-*cis*-$C_2H_2Me_2$) (1-*cis*-$C_2H_2Me_2$).** After heating for 16 h at 85 °C, isolation from pentane afforded 75 mg of dark green **1**-*cis*-$C_2H_2Me_2$ (40%). **e. (silox)$_3$Nb(η-$C_2H_3C_6H_4$-*p*-OMe) (1-C_2H_3Ph-*p*-OMe).** After being stirred for 18 h at 23 °C, isolation from diethyl ether afforded 170 mg of green-brown **1**-C_2H_3Ph-*p*-OMe (46%). Anal. Calcd for $C_{45}H_{91}Si_3O_4Nb$: C, 61.89; H, 10.50. Found: C, 61.70; H, 10.71. **f. (silox)$_3$Nb(η-$C_2H_3C_6H_4$-*p*-CF_3) (1-C_2H_3Ph-*p*-CF_3).** After being stirred for 18 h at 23 °C, isolation from diethyl ether afforded 170 mg of army green **1**-C_2H_3Ph-*p*-CF_3 (44%).

3. (silox)$_3$Nb(ole) (1-ole) from (silox)$_3$Nb(PMe$_3$) (1-PMe$_3$). Into a flask charged with (silox)$_3$NbPMe$_3$ (**1**-PMe$_3$), 25 mL of pentane and excess olefin were distilled. The reaction mixture was stirred for variable times and temperatures, transferred to a flask, and crystallized. **a. (silox)$_3$Nb(η-C_2H_3^{t}Bu) (1-C_2H_3^{t}Bu).** After stirring **1**-PMe$_3$ with ∼20 equiv of C_2H_3^{t}Bu for 2 h at 23 °C, isolation from diethyl ether afforded 342 mg of brown microcrystalline **1**-C_2H_3^{t}Bu (90%). Anal. Calcd for $C_{42}H_{93}Si_3O_3Nb$: C, 61.27; H, 11.39. Found: C, 60.23; H, 11.33. **b. (silox)$_3$Nb(η-^{c}C$_5$H$_8$) (1-^{c}C$_5$H$_8$).** After stirring **1**-PMe$_3$ with ∼35 equiv of ^{c}C$_5$H$_8$ for 2 h at 23 °C, isolation from diethyl ether afforded 130 mg of green microcrystalline **1**-^{c}C$_5$H$_8$ (50%). Anal. Calcd for $C_{41}H_{89}Si_3O_3Nb$: C, 60.00; H, 11.11. Found: C, 61.06; H, 11.13.

4. (silox)$_3$Nb(ole) (1-ole) from (silox)$_3$NbCl$_2$ (3). Into a flask charged with **3** and 2.1 equiv of 0.65% Na/Hg, THF and excess olefin were condensed at 77 K. After being stirred for 12 h, the THF was removed and replaced with hydrocarbon solvent. The solution was filtered, and the complex was crystallized. **a. (silox)$_3$Nb(η-^{c}C$_6$H$_{10}$) (1-^{c}C$_6$H$_{10}$).** Crystallization from hexanes provided 600 mg of dark green **1**-^{c}C$_6$H$_{10}$ (40%). Anal. Calcd for $C_{42}H_{91}Si_3O_3Nb$: C, 61.42; H, 11.17. Found: C, 61.19; H, 11.02. **b. (silox)$_3$Nb(η-^{c}C$_7$H$_{10}$) (1-^{c}C$_7$H$_{10}$).** Crystallization from diethyl ether afforded 253 mg of green microcrystalline **1**-^{c}C$_7$H$_{10}$ (25%).

5. (silox)$_3$Ta(ol) (2-ole). General. A flask or bomb reactor (in the case of gaseous olefins) was charged with (silox)$_3$Ta (**2**), a hydrocarbon solvent, and an excess of olefin. After being stirred for a period of time at 23 °C, the blue color changed to orange, the solvent was removed, and the yellow-orange to red solid was triturated, dissolved in hexanes, and filtered. Crystallization was typically from hexanes or diethyl ether at −78 °C. **a. (silox)$_3$Ta(η-C_2H_3Et) (1-C_2H_3Et).** After being stirred for 1 h at 23 °C, 200 mg of orange **1**-C_2H_3Et was crystallized from pentane (67%). Anal. Calcd for $C_{40}H_{89}Si_3O_3Ta$: C, 54.39; H, 10.16. Found: C, 54.23; H, 10.17. **b. (silox)$_3$Ta(η-^{c}C$_5$H$_8$) (2-^{2}C$_5$H$_8$).** After being stirred for 1 h at 23 °C, 222 mg of orange **2**-^{c}C$_5$H$_8$ was crystallized from diethyl ether (63%). **c. (silox)$_3$Ta(η-^{c}C$_6$H$_{10}$) (2-^{c}C$_6$H$_{10}$).** After being stirred for 24 h at 23 °C, 186 mg of orange **2**-^{c}C$_5$H$_8$ was crystallized from diethyl ether (55%). **d. (silox)$_3$Ta(η-^{c}C$_7$H$_{10}$) (2-^{c}C$_7$H$_{10}$).** After being stirred for 12 h at 23 °C, 145 mg of orange **2**-^{c}C$_7$H$_{10}$ was crystallized from diethyl ether (47%). Anal. Calcd for $C_{43}H_{91}Si_3O_3Ta$: C, 56.03; H, 9.95. Found: C, 55.90; H, 9.85. **e. (silox)$_3$Ta(η-C_2H_3Ph) (2-C_2H_3Ph).** After being stirred for 1 h at 23 °C, 195 mg of orange **2**-C_2H_3Ph was crystallized from pentane (65%). Anal. Calcd for $C_{43}H_{91}Si_3O_3Ta$: C, 56.74; H, 9.63. Found: C, 56.05; H, 9.64. **f. (silox)$_3$Ta(η-$C_2H_3C_6H_4$-*p*-OMe) (2-C_2H_3Ph-*p*-OMe).** After being stirred for 1 h at 23 °C, 195 mg of red **2**-C_2H_3Ph-*p*-OMe was crystallized from pentane (62%). **g. (silox)$_3$Ta(η-$C_2H_3C_6H_4$-*p*-CF_3) (2-C_2H_3Ph-*p*-CF_3).** After being stirredfor 1 h at 23 °C, 180 mg of orange **2**-C_2H_3Ph-*p*-CF_3 was crystallized from pentane (55%).

6. (silox)$_3$Nb=CH^{n}Pr (1=CH^{n}Pr). A 50-mL bomb charged with 350 mg of **1**-C_2H_3Et (0.440 mmol) and 20 mL of benzene was heated at 155 °C for 8.5 h. Upon cooling a diethyl ether solution to −78 °C, 90 mg of microcrystalline red **1**=CH^{n}Pr was obtained (26%). Anal. Calcd for $C_{40}H_{89}Si_3O_3Nb$: C, 60.41; H, 11.28. Found: C, 60.19; H, 11.42.

7. (silox)$_3$Nb=^{c}C$_6$H$_{10}$ (1=^{c}C$_6$H$_{10}$). A 50-mL bomb charged with 600 mg of **1**-^{c}C$_6$H$_{10}$ (0.732 mmol) and 25 mL of benzene was heated at 55 °C for 13 d. Upon cooling a pentane solution to −78 °C, 415 mg of dark green microcrystalline **1**=^{c}C$_6$H$_{10}$ was obtained (69%). Anal. Calcd for $C_{42}H_{91}Si_3O_3Nb$: C, 61.60; H, 11.90. Found: C, 60.91; H, 11.84.

8. (silox)$_3$^{n}BuTa(κ^2-O,C-OSi^{t}Bu$_2$CMe$_2$CH$_2$) (6-^{n}Bu). An NMR tube was charged with 180 mg of **1**-C_2H_3Et (0.204 mmol) and 1 mL of toluene-d_8. After being heated for 12 h at 103 °C, the solution was pale yellow. The solvent was allowed to evaporate over the course of 7 d to give 90 mg of **6**-^{n}Bu (50%) as a crystalline solid. Anal. Calcd for $C_{40}H_{89}Si_3O_3Ta$: C, 54.39; H, 10.16. Found: C, 53.86; H, 9.69.

NMR Tube Reactions. Flame-dried NMR tubes, sealed to 14/20 ground glass joints, were charged with the organometallic reagent (typically 20 mg) and any other solid reagent in a drybox and removed to the vacuum line on needle valve adapters. The NMR tube was degassed, and after transfer of deuterated solvent, a calibrated gas bulb was used to introduce volatile reagents at 77 K if necessary. The tubes were then sealed with a torch. Sometimes freshly distilled solvent was added to the tubes while in the drybox, then moved to the vacuum line, degassed, and sealed with a torch.

Kinetics Studies. Sets of three and six NMR tubes for kinetics monitoring of the olefin to alkylidene isomerization were prepared as described above. Once the solution was added to the NMR tubes, they were transferred to the vacuum line attached to a 3- or 6-prong adapter, evacuated and sealed. Kinetics experiments were typically done in sets of three for adequate statistics. The sets of NMR tubes were placed simultaneously in a temperature-controlled oil bath for a measured amount of time and periodically removed, frozen at 77 K, and warmed and analyzed by ^{1}H NMR spectroscopy. For the specific resonances monitored, see Supporting Information.

Kinetics Modeling. All experimental data were analyzed using Scientist 2.0 by MicroMath for Microsoft Windows. Least squares regression analyses were employed to model all forward and reverse rate constants as well as activation parameters via the Eyring equation.

Equilibrium Studies. General. NMR tubes for measuring the equilibria listed in Table 3 were prepared as described above. After equilibrium was achieved, integration of appropriate ^{1}H NMR spectroscopic resonances afforded equilibrium constants. Specific resonances analyzed are given in the Supporting Information.

Single-Crystal X-ray Diffraction Studies. A crystal was isolated, covered in polyisobutylene, and placed under a 173 °C N_2 stream on the goniometer head of a Siemens P4 SMART CCD area detector system (graphite-monochromated Mo Kα radiation, $\lambda = 0.71073$ Å). The structure was solved by direct methods (SHELXS). All non-hydrogen atoms were anisotropically refined, and hydrogen atoms were treated as idealized contributions.

9. (silox)$_3$Nb=^{c}C$_6$H$_{10}$) (1-^{c}C$_6$H$_{10}$). Dark green crystals of **1**-^{c}C$_6$H$_{10}$ were grown from evaporating a concentrated benzene-d_6 solution. In space group *Pca*2$_1$, correlation problems are known to interfere with

normal refinement if a local center of symmetry is near $x = 1/8$ and $y = 1/4$.[98] Two local centers of symmetry at $x = 0.85$, $y = 0.749$ and $x = 0.860$, $y = 1.249$ were found. Even greater problems may arise if some of the atoms have special values for y (0.0 and 0.5 for a pair of related atoms).[98] Note that the atom coordinates of the niobiums meet these criteria (atom, *x*, *y*, *z*: Nb1, 0.7468, 0.50578, 0.345; Nb1A, 0.9614, 0.9921, 0.4100; Nb1B, 0.7607, 1.0057, 0.6587; Nb1C, 0.9614, 1.4929, 0.5973). In this structure, eight of nine *tert*-butyl groups are related by a local inversion center; hence, while the structure is correctly refined in a noncentrosymmetric space group, it is very nearly centrosymmetric, leading to some problems of correlation. Refinement in the centrosymmetric space group *Pbca* afforded an R_1 of ~16%. The average values of bond lengths and angles are reported for this molecule because they should be unaffected by this pseudo-symmetry.

10. (silox)$_3$Ta(η-C$_2$H$_3$Et) (2-C$_2$H$_3$Et). Bright orange crystals of **2**-C_2H_3Et were grown from evaporating a concentrated benzene solution.

11. (silox)$_3$^{n}BuTa(κ^2-O,C-OSi^{t}Bu$_2$CMe$_2$CH$_2$) (6-^{n}Bu). A light yellow crystal of **6**-^{n}Bu from procedure 8 was used. The *tert*-butyl groups of one silox (Si3) were disordered, and each was treated as two units of half-occupancy.

Calculations. To obtain the minima in this research, full geometry optimizations—without any metric or symmetry restrictions—were performed using the Gaussian[99] package, and these employed density functional theory, specifically the BLYP functional.[100] Atoms were described with the Stevens effective core potentials and attendant valence basis sets.[101] This scheme, dubbed CEP-31G(d), entails a valence triplet ζ description for the transition metals, a double-ζ-plus-polarization basis set for main group elements, and the −31G basis set for hydrogen. This level of theory was selected on the basis of a series of test calculations on the singlet and triplet states of $Nb(OH)_3$ (**1′**), $Ta(OH)_3$ (**2′**),[38] and their olefin adducts.

Acknowledgment. This research is dedicated to the memory of Ian P. Rothwell, a great friend and colleague, and a master of group 5. Support from the National Science Foundation (P.T.W., CHE-0212147; T.R.C., CHE-0309811) and Cornell University is gratefully acknowledged. Profs. Barry K. Carpenter, Charles F. Wilcox, David B. Collum, Kit Cummins, and Richard Marsh are thanked for helpful discussions.

Supporting Information Available: Crystallographic data (CIF), a detailed experimental description, and a discussion of entropy of activation estimations (PDF). This material is available free of charge via the Internet at http://pubs.acs.org.

JA046180K

(98) Marsh, R. R.; Schomaker, V.; Herbstein, F. H. *Acta Crystallogr.* **1998**, *B54*, 921−924.

(99) Frisch, M. J.; Trucks, G. W.; Schlegel, H. B.; Scuseria, G. E.; Robb, M. A.; Cheeseman, J. R.; Zakrzewski, V. G.; Montgomery, J. A., Jr.; Stratmann, R. E.; Burant, J. C.; Dapprich, S.; Millam, J. M.; Daniels, A. D.; Kudin, K. N.; Strain, M. C.; Farkas, O.; Tomasi, J.; Barone, V.; Cossi, M.; Cammi, R.; Mennucci, B.; Pomelli, C.; Adamo, C.; Clifford, S.; Ochterski, J.; Petersson, G. A.; Ayala, P. Y.; Cui, Q.; Morokuma, K.; Malick, D. K.; Rabuck, A. D.; Raghavachari, K.; Foresman, J. B.; Cioslowski, J.; Ortiz, J. V.; Stefanov, B. B.; Liu, G.; Liashenko, A.; Piskorz, P.; Komaromi, I.; Gomperts, R.; Martin, R. L.; Fox, D. J.; Keith, T.; Al-Laham, M. A.; Peng, C. Y.; Nanayakkara, A.; Gonzalez, C.; Challacombe, M.; Gill, P. M. W.; Johnson, B. G.; Chen, W.; Wong, M. W.; Andres, J. L.; Head-Gordon, M.; Replogle, E. S.; Pople, J. A. *Gaussian 98*, revision x.x; Gaussian, Inc.: Pittsburgh, PA, 1998.

(100) Parr, R. G.; Yang, W. Density-Functional Theory of Atoms and Molecules; Oxford University Press: Oxford, 1989.

(101) Stevens, W. J.; Krauss, M.; Basch, H.; Jasien, P. G. *Can. J. Chem.* **1992**, *70*, 612−630.